TEMPERATURE DEPENDENCE OF LINE WIDTHS

OF THE INVERSION SPECTRA OF AMMONIA

APPROVED:

James A. Robert
Major Professor

Russell H Bilyeu
Minor Professor

L F Bonnell Jr
Director of the Department of Physics

Robert B. Toulouse
Dean of the Graduate School

TEMPERATURE DEPENDENCE OF LINE WIDTHS OF THE INVERSION SPECTRA OF AMMONIA

THESIS

Presented to the Graduate Council of the
North Texas State University in Partial
Fulfillment of the Requirements

For the Degree of

MASTER OF SCIENCE

By

Charles E. Cook, B.S.
Denton, Texas
August, 1969

TABLE OF CONTENTS

LIST OF TABLES

LIST OF ILLUSTRATIONS

CHAPTER I

INTRODUCTION

One of the purposes of this work is to investigate modifications that have to be made to a standard source-modulation microwave spectograph so that it can be used to study gases at various temperatures. Specific modifications as well as limitations are discussed in Chapter III. Another objective in this work is to determine experimentally the function of temperature that describes how the line widths of microwave spectral lines vary with changing temperature. The most important segment of the study is the temperature dependence of the line width since from an accurate knowledge of this temperature dependence one is able to determine what molecular force fields are present and the relative importance of parts of the molecular force field.

The curve describing the line half width, $\Delta\nu$, as a function of temperature is given by the following equation,

$$T^{[(n-3)/2(n-1)]}, \qquad [I-1]$$

where T = absolute temperature.

n = some positive integer depending on the molecular force field.

This result, which assumes a fixed number of molecules in the absorption cell, is developed in Chapter II.

If one can experimentally confirm a certain value for n then, as will be shown in Chapter II, the variation of interaction energy between the "colliding" molecules is proportional to $1/r^n$, where r is the separation of the two molecules. This result assumes one predominant interaction potential. For example, if n = 3, the type of interaction is dipole-dipole. Table I shows some of the various values n might have, the corresponding type of interaction, and the predicted temperature dependence. Note that the $1/r^2$ and 1/r interactions are omitted. No well known potential has a $1/r^2$ dependence. The 1/r (Coulomb) potential is omitted since only non-ionized molecules are considered.

Figure 1 shows a plot of the half width, $\Delta\nu$, versus the absolute temperature for three types of interactions given in Table I. It is easily seen that unless the experimental data are quite accurate one would be unable to state accurately the temperature dependence.

The particular spectrograph used in this study has a lower limit on the resolution of about 2 per cent of the total line width. Therefore, the resolution needed to distinguish between the different curves in Figure 1

is easily supplied by the spectrograph. If the temperature and other variables are accurately known, it is indeed possible to distinguish between the curves giving different temperature dependences.

During the first half of the 1950's there was some work done on this subject. Because of many difficulties, since that time there has been relatively little work done on the temperature dependence of microwave line widths. These early workers covered a greater temperature range than is covered in this study. (2,3,8,9,10) Their studies differ in three ways from this one. First, their temperatures were generally much higher than room temperature. The highest temperature used by Feeny et al. was 500° K. The high temperatures were varied continuously. The only temperature below room temperature was 195 °K. Second, the spectrographs used were inferior in resolution to that used in this study because of the infancy of the microwave field. Third, from the rather sketchy journal articles, it is doubtful that these workers took into account the adsorption of the gas being studied onto the walls of the absorption cell.

Thus far nothing has been said about the type of microwave lines being investigated. The lines studied here are exclusively inversion lines of ammonia (NH_3),

which is a symmetric-top molecule. The following qualitative discussion will concern the ammonia molecule. The problem has been treated quantitatively by Dennison and Uhlenbeck. (1)

The ammonia molecule has a configuration as shown in Figure 2. It has a pyramidal structure, with the three hydrogen atoms forming the base plane. The molecule is capable of absorbing energy and distributing that energy into its allowed degrees of freedom which include rotational, vibrational, and translational modes. Each of these modes of activity can be studied by using different energies to stimulate the molecule. Since this investigation is concerned primarily with the rotational and inversion (vibrational) levels of molecules that lie in the microwave-frequency region, a discussion of the inversion spectra of ammonia is worthwhile. It will be advantageous for a better understanding of later discussions to discuss the rotational-energy levels of symmetric-top rotors since these serve as a basis for inversion levels. In a semi-classical way one may arrive at the energy levels. Classically the total energy of rotation may be written as

$$E = \frac{L_x^2}{2I_x} + \frac{L_y^2}{2I_y} + \frac{L_z^2}{2I_z}, \qquad [I\text{-}2]$$

where L_x, L_y, L_z = the respective x, y, z components of angular momentum, and

I_x, I_y, I_z = the respective moments of inertia about the x, y, z axes.

For convenience the z axis is chosen to lie along the axis of symmetry. Since the molecule is a symmetric top, I_x and I_y are equal and will both be called I_B. Using $I_x = I_y = I_B$ and the fact that the total angular momentum, L^2, is equal to $L_x^2 + L_y^2 + L_z^2$, Equation [I-2] becomes

$$E = \frac{L^2}{2I_B} + L_z^2 \left[\frac{1}{2I_2} - \frac{1}{2I_B}\right] . \qquad [I-3]$$

The square of the total angular momentum is found quantum-mechanically to be $J(J+1)h^2$, where J is an integer. Similarly, L_z^2 is quantized and must have the value K^2h^2, where K is also an integer. Since the quantum number K represents the projection of the angular momentum along the molecular symmetry axis, the usual restriction $J \geq |K|$ applies. Using these quantized momenta and defining the following constants

$$B = \frac{h}{8\pi^2 I_B} \quad \text{and} \quad C = \frac{h}{8\pi^2 I_z} , \qquad [I-4(a)]$$

the energy may be written as

$$E = [BJ(J+1) + (C-B)K^2]h. \qquad [I-4(b)]$$

This same energy is obtained in a more rigorous way by solving the following equation: (4)

$$\frac{1}{\sin\theta}\frac{\partial}{\partial\theta}\left(\sin\theta\frac{\partial\psi}{\partial\theta}\right) + \frac{1}{\sin^2\theta}\frac{\partial^2\psi}{\partial\phi^2} + \left(\frac{\cos^2\theta}{\sin^2\theta} + \frac{C}{B}\right)\frac{\partial^2\psi}{\partial\chi^2} - \frac{2\cos\theta}{\sin^2\theta}\frac{\partial^2\psi}{\partial\chi\partial\phi} + \frac{E\psi}{hB} = 0. \qquad [I-5]$$

This is the wave equation in terms of Euler's angles. θ and ϕ are equivalent to the usual polar angles and χ is the angle of rotation around the axis of symmetry fixed in the molecule.

For the present discussion one of the main points of consideration is that for a particular energy level there are corresponding values for the quantum numbers J and K. Even more important is that for given values of J and K one knows the rotational configuration of the molecule and can infer something about the centrifugal distortion of the molecule. In other words, for different sets of quantum numbers J and K, the basic configuration of the molecule is the same but the values of l and θ shown in Figure 2 will vary as a consequence of the centrifugal distortion. It is customary to give the rotational state of a molecule by stating the quantum numbers of the state function. For example, a molecule having the quantum numbers $J = 7$ and $K = 3$ has its rotational state denoted by (7,3). The need for a realization of this centrifugal distortion will be seen shortly.

When considering the inversion spectra of ammonia, one in reality considers the vibration of the nitrogen atom along a line perpendicular to the hydrogen plane. Figure 3 shows the NH_3 molecule from a different point of view than that in Figure 2, and also the accompanying

potential "seen" by the nitrogen atom. A qualitative feeling for the energy levels can be obtained from a study of the series of diagrams in Figure 4. In Figure 4 the variations of the energy levels with the barrier height are depicted. From the diagrams it is seen that as the barrier grows the energy levels of the unperturbed harmonic oscillator will begin to coalesce by pairs into single energy levels. This happens only below V_b. On the other hand, if one looks at the two nearby oscillator potentials as in Figure 5(A), it can be imagined what happens, as the barrier between them gets lower as in Figure 5(B). It is observed that the energy levels of the two separate oscillators split as the barrier height, V , decreases. The gap between successive split levels increases with energy as shown.

Transitions that are between one of the two levels in group 1 of Figure 5(B) and a level in group 2, or higher energy levels, correspond to energies that have frequencies in the infrared. This fact is of little interest to the microwave spectroscopist, as it lies above the range of presently available equipment. However, transitions between the two levels in group 1 have frequencies that lie in the microwave region. These are the so called "inversion transitions." This type of transition is not due to the nitrogen tunneling through the barrier, which

is allowed quantum-mechanically, but is simply due to a transition between vibrational states. These two vibrational states (group 1 in Figure 3(B)) are there as a consequence of solutions of the Schroedinger wave equation.

The misnomer "inversion line" creeps in due to the fact that quantum-mechanically it can be shown that the nitrogen tunnels through the barrier with a frequency corresponding to the energy separation of the two energy levels in group 1 of Figure 3(B). This inversion process affects the energy levels in no way. The energy levels split or coalesce, depending on the point of view taken, according to permissible solutions of the Schroedinger equation for this kind of potential. The fact that this event occurs simultaneously with inversion should not be construed to mean that one process "causes" the other. They simply occur simultaneously.

The frequency of an inversion spectral line for NH_3 is of course dependent upon the barrier height. This height is in turn dependent upon how the molecule is rotation. So, if one desires to speak meaningfully about the inversion transition for an NH_3 molecule, its angular momentum comfiguration must first be specified by giving the set of quantum numbers J and K. Throughout the rest of this work, inversion lines of a particular molecule

will be denoted by this pair of quantum numbers.

A description of the microwave spectrometer used for this study follows closely that given by Rinehart et al. (6) However, certain improvements have been made. These improvements and a general description of the particular spectrograph used are described by Roberts. (7) For this temperature study the basic spectrograph of Roberts was used with two notable changes. Instead of a coiled circular waveguide, a thermally insulated coiled rectangular waveguide was used. Also, the pressure-measuring system was different. These aspects were discussed fully in Chapter III.

Figure 6 shows the spectrograph in the form of a block diagram. The klystron has well regulated voltages applied to it. It is made to sweep through a range of frequencies that can be made to include the inversion line by periodically applying a sawtooth voltage to the repeller. The sawtooth voltage is supplied by an oscilloscope that is used as part of the display, or readout. This sawtooth provided by the oscilloscope produces synchronization of the display on the oscilloscope with the output of the klystron.

Superimposed upon the sawtooth signal, whose frequency is usually about .02 hertz, is a 43 kilohertz square wave supplied by the upper of the two modulators

shown in Figure 6. The effect of this modulation is to produce the derivative of the line shape on the readout device. The power "observed" by the detector-amplifier system will not appear as in Figure 7(A), but as in Figure 7(B). Figure 7(A) is the assumed shape of the absorption line, while Figure 7(B) is effectively its derivative. The variation in power that the detector and amplifiers at the end of cell "see" is that shown in Figure 7(B).

There are three principal reasons for using the derivative of the line shape rather than the line shape itself. First, the points on the derivative that correspond to the points of steepest slope on the line are easier to locate than are the half-power points on the line itself. (The line width, $2\Delta\nu$, is defined as the frequency spacing between the half-power points.) Figure 8 illustrates the relation between the line shape and its derivative. Experimentally, one measures the distance between the peaks of the derivative. These can be more accurately located than the corresponding points of steepest slope on the line shape. Formulas have been developed giving the relationship between $\Delta\nu$ and $\delta\nu$. (5) These two quantities are depicted in Figure 8.

Second, the excursion of the voltage at the detector is not as great. Hence the nonlinearity of the amplifiers

system does not produce as much distortion as it would when the line shape is amplified directly.

Third, amplification of the signal is easier. The amplifier is tuned for 45 kilohertz, the frequency of the upper modulator in Figure 6, and this frequency is much easier to amplify selectively by tuning than the slowly varying sweep which yields the line shape.

As is indicated in the block diagram in Figure 6, a portion of the microwave power from the klystron is tapped off and sent to a mixer, where it is mixed with standard frequencies. An interpolation receiver is also connected to the mixer and tuned to the appropriate frequency. This arrangement yields "markers" that are displayed simultaneously on a dual-pen chart recorder with the line-shape derivative. Since the frequency spacing of the markers is known, this display serves as a basis for measuring the frequency separation of the peaks of the derivative. Figure 9 is a typical display on the chart recorder.

A more detailed discussion of some of the techniques listed above will be given in the chapter on experimental procedure. In that chapter, experimental procedures and instrumentation unique to this temperature study will be discussed.

CHAPTER BIBLIOGRAPHY

1. Dennison, D. M. and Uhlenbeck, G. E., "The Two-Minima Problem and the Ammonia Molecule," Physical Review, XLI (August, 1932), 313-321.

2. Feeny, H., Lackner, H., Moser, Paul, and Smith, W.V., "Pressure Broadening of Linear Molecules," The Journal of Chemical Physics, XXII (January, 1953), 79-83.

3. Johnson, C. M. and Slager, D. M., "Line Breadth of OCS as a Function of Rotational Transition and Temperature," Physical Review, LXXXVII (August, 1953), 677-678.

4. Kemble, E. C., The Fundamental Principles of Quantum Mechanics, New York, McGraw-Hill Co., Inc., 1937.

5. Rinehart, E. A., Kleen, R. H., Lin, C. C., "Measurement of the Widths of Microwave Spectral Lines," Journal of Molecular Spectroscopy V (December, 1960), 458-473.

6. Rinehart, E. A., Legan, R. L., Lin, Chun C., "Microwave Spectrograph for Line Width Measurements," Review of Scientific Instruments, XXXVI (April, 1965), 511-517.

7. Roberts, J. A., "An Improved Microwave Spectrometer for Linewidth Measurements," (To be published) Review of Scientific Instruments.

8. Smith, W. V., and Howard, R. R., "Microwave Collision Diameters II. Theory and Correlations with Molecular Quadrupole Moments," Physical Review, LXXIX (July, 1950), 132-136.

9. _____, "Temperature Dependence of Microwave Line Widths," Physical Review, LXXVII (March, 1950), 840-841.

10. Smith, W. V., Lackner, H.A., and Volkov, A.B., "Pressure Broadening of Linear Molecules II. Theory," The Journal of Chemical Physics, XXIII (February, 1955), 389-396.

CHAPTER II

THEORETICAL TEMPERATURE DEPENDENCE OF LINE WIDTHS

The sources of microwave spectral line broadening fall under six main headings. They are natural line breath, Doppler effect, wall broadening, saturation broadening, nearby lines, and pressure broadening. This chapter contains the results of a theoretical investigation of the temperature dependence of each of these as they apply specifically to microwave spectral lines.

Natural Line Breadth

Natural line breadth may be interpreted quantum mechanically as a disturbance of the molecule by zero-point vibrations of electromagnetic fields. It is desirable to find first an expression for the line width of a transition from some arbitrary state to the ground state as a result of these zero-point electromagnetic field vibrations. In a semiclassical way the transition probability per unit time for spontaneous emission of an electric dipole is found to be (6)

$$\text{prob./time} = (32\pi^3\nu^3/3hc^3)\ |\mu|^2, \qquad [\text{II-1}]$$

where ν = frequency of perturbing radiation, and
μ = matrix element of the dipole moment.

It is reasonable to associate the rate of decrease of energy of a classical oscillator with the rate of decrease of the probability of finding the corresponding quantum system in its initial upper state. If this is done, the quantum analog of the classical natural line breadth, $2\Delta\nu$, is the initial transition probability per unit time for spontaneous emission given in Equation [II-1]. Hence, one expects the line width due to zero point electromagnetic radiation to be

$$2\Delta\nu = 2(32\pi^3\nu^3/3hc^3)\ |\mu|^2. \qquad [II-2]$$

The term "zero-point" above has the implication that Equation [II-2] is good only for a temperature of absolute zero. The required task is to find the line half width, $\Delta\nu$, for temperatures other than $T = 0^\circ K$. To achieve this, the basic assumption is made that the line width is proportional to the energy of the oscillator producing the radiation that induces the transition.

At $T = 0^\circ K$ one may assume this radiation originates from three-dimensional harmonic oscillators in the ground state. Of course, the transition induced by this radiation is equal in frequency to the frequency of the perturbing radiation. In the ground state a quantum of excitation of one of these three-dimensional oscillators has energy equal to $3(n + \frac{1}{2})h = 3/2\ h$ since $n = 0$ in the ground state.

Now consider what effect the radiation from these oscillators has at some higher temperature. Consider temperatures sufficiently high so that the equipartation theorem may be used. Each three-dimensional oscillator will have an amount of energy given by

$$E = 3(\text{K.E.} + \text{P.E.}) = 3(\tfrac{1}{2}kT + \tfrac{1}{2}kT) = 3kT, \quad [\text{II-3}]$$

where K.E. = kinetic energy of one dimension,
P.E. = potential energy of one dimension,
k = Boltzmann's constant, and
T = absolute temperature.

The ratio of the two energies discussed above can be used to determine how much more effective the higher temperature oscillators are in broadening the line. That ratio is given by $2kT/h\nu$.

For natural line widths at sufficiently high temperatures, the right side of Equation [II-2] should be multiplied by this factor. Hence, the natural line half width as a function of temperature is written as

$$= (2kT/h\nu)\ (32\pi^3\nu^3/3hc^3)\ |\mu|^2. \quad [\text{II-4}]$$

This equation is for transitions whose lower energy level is the ground state. In the inversion spectra of ammonia studied in this work, the lower energy level involved in a transition is the ground state. For NH_3 the inversion line in the microwave range is between the two levels in group 1 of Figure 3(B). Equation [II-4] applies in this study because the temperatures used were high enough to

make the equipartition theorem valid. Temperatures low enough to invalidate Equation [II-4] are also low enough to liquefy NH_3 at a few microns of pressure.

For room temperatures, the natural width given by Equation [II-4] is of the order of 10^{-5} hertz and is quite negligible when compared to other types of broadening; in fact, it is immeasurably small with presently available spectrographs.

Doppler Effect

It is known that the shape of a spectral line, the plot of the intensity (I) versus the frequency (ν) of the perturbing radiation, is a function of temperature T and the line width $\Delta\nu$. Here the Doppler effect is inserted and an additional temperature dependence results.

Consider a source of radiation of frequency ν and some molecules that form a gas. The molecules, being at absolute temperature T, will have random velocities with respect to the incoming radiation and as a result they will "observe" the radiation as having a frequency $\nu' \neq \nu$. From the theory of special relativity, one is able to calculate ν' in terms of ν with the following two formulas:

$$\nu' = \nu\left[\frac{1 + V_x/c}{1 - V_x/c}\right]^{\frac{1}{2}}, \qquad \begin{matrix}\text{Longitudinal Doppler} \\ \text{effect}\end{matrix} \quad [II-5]$$

$$\nu' = \nu\left[1 - (V_T/c)^2\right]^{\frac{1}{2}}, \qquad \text{Transverse Doppler Effect} \quad [II-6]$$

where V_x = relative velocity of approach between "observer" and source. V_x is positive if they approach, and
V_T = relative component of velocity perpendicular to the line joining the source and observer.

For the highest temperature used in this study (about 350°K), the velocity of NH_3 molecules is sufficiently small that Equation [II-6] may be neglected and Equation [II-5] can be approximated by keeping the first two terms of its binomial expansion. Equation [II-5] thus becomes

$$\nu' \simeq \nu(1 + V_x/c), \qquad [II-7]$$

so that the shift in frequency that a molecule observes is

$$\nu' - \nu = V_x/c \ . \qquad [II-8]$$

How does one go about inserting the Doppler effect given by Equation [II-8] into the expression for the shape of a line that already has a non-zero width, $\Delta\nu$? First of all, consider the line shape without the Doppler effect. This is the well-known Van Vleck-Weisskopf equation and is given by

$$I = \frac{8\pi^2 Nf}{3ckT}\,|\mu_{ij}|^2\,\nu^2\left[\frac{\Delta\nu}{(\nu-\nu_o)^2+(\Delta\nu)^2} + \frac{\Delta\nu}{(\nu+\nu_o)^2+(\Delta\nu)^2}\right], \qquad [II-9]$$

where N = the number of molecules per unit volume,
f = fraction of the total number of absorbers, in the lower of the two states involved, in the transition,
ν_o = proper frequency of the transition, and
$|\mu_{ij}|$ = dipole matrix element for the transition $i \longleftrightarrow j$.

Replacing Nf by n, the number of molecules per unit volume in the lower state, and realizing that at microwave frequencies $\Delta\nu \ll \nu_o$, the second term in brackets of Equation [II-9] may be neglected and one finds

$$= \frac{8\pi^2 n}{3ckT} |\mu_{ij}|^2 \nu^2 \frac{\Delta\nu}{(\nu - \nu_o)^2 + (\Delta\nu)^2} . \quad [II-10]$$

The assumption that $\Delta\nu \ll \nu_o$ is a good one because the frequencies of the spectral lines investigated were large compared to the line widths. Only relatively narrow lines were studied since for wide ones the critical points are difficult to resolve. Of course, studying wide lines leads to large errors in line widths measurements.

The Doppler effect is introduced into Equation [II-10] through n. The quantity n can be related to the Doppler effect through the Maxwellian distribution of molecular velocities. The Maxwellian distribution is given by

$$\delta n_{v_x} = N(m/2\pi kT)^{\frac{1}{2}} \exp(-mV_x^2/2kT)\delta V_x, \quad [II-11]$$

where n_{v_x} is the number of molecules per unit volume having an x-component of velocity in the range $V_x \longrightarrow V_x + dV_x$.

Combining Equations [II-8] and [II-11] yields

$$\delta n_{v_x} = n(m/2\pi kT)^{\frac{1}{2}} \exp[-mc^2(\nu' - \nu)^2/2kT\nu^2]. \quad [II-12]$$

Substituting n_{v_x} of Equation [II-12] for n in Equation [II-10] would yield the contribution this small number of molecules makes to the intensity. Integrating over the full range of V_x gives the total intensity of the line as a function of ν and is written as

$$\frac{8\pi^2 n}{3ckT}\left[\frac{m}{2\pi kT}\right]^{\frac{1}{2}} |\mu_{ij}|^2 \Delta\nu \int_{-\infty}^{\infty} \nu'^2 \frac{\exp[-mc^2(\nu'-\nu)^2/2kT\nu'^2]}{(\nu' - \nu_o)^2 + (\Delta\nu)^2} \delta V_x. \quad [II-13]$$

Note that before combining Equation [II-10] and [II-12], ν in Equation [II-10] was replaced by ν', the frequency "observed" by the molecule. A more convenient form for integration is obtained by making the substitution $V_x = (c/\nu)d\nu'$. This comes from Equation [II-8] and a realization that ν is treated as a constant since only the variation of ν' with V_x is considered. Thus Equation [II-13] may be written as

$$I = 4/3(2m)^{\frac{1}{2}}(\pi/kT)^{3/2} n|\mu_{ij}|^2 \Delta\nu/\nu \int_{-\infty}^{\infty} \nu'^2 \frac{\exp[-mc^2(\nu'-\nu)^2/2kT\nu'^2]}{(\nu'-\nu_o)^2 + (\Delta\nu)^2} d\nu'. \quad [II-14]$$

Since n has served its purpose for bringing in the Doppler effect via the Maxwellian distribution, it may be replaced by $Ce^{-W_o/kT}$ to show its temperature dependence.

Here C is a constant and W_o is the energy of the lower state. Simultaneously with this substitution the integral can be considerably simplified by making the approximation $\nu'^2/\nu \simeq \nu^2/\nu \simeq \nu_o$. This is justifiable since ν' is not much different from ν and because the intensity of the line is appreciable only in the "neighborhood" of ν_o. The intensity may now be written as

$$I(\ ) = C\frac{\exp(-W_o/kT)}{T^{3/2}}\,\nu_o\,\Delta\nu\int_{-\infty}^{+\infty}\frac{\exp[-mc^2(\nu'-\nu)^2/2kT\nu^2]}{(\nu'-\nu_o)^2+(\Delta\nu)^2}\,d\nu'. \qquad [II\text{-}15]$$

Now look at the actual line width, designated ΔW, calculated from Equation [II-15]. The line half width can be broken down into three sections, the case where $\Delta\nu$ is very small, where it is relatively large, and intermediate values. At this point, it is well to point out that $\Delta\nu$ in Equation [II-15] is not the width of the Doppler corrected line, but the width of the uncorrected line. Therefore, the limit as $\Delta\nu \to 0$ can be meaningfully taken.

Small $\Delta\nu$

When collision broadening is insignificant, then $\Delta\nu$ is small. This problem could be solved by taking the limit as $\Delta\nu \to 0$ in Equation [II-15]. Perhaps an easier method of finding this pure Doppler line shape is to go back to more basic ideas. It is no longer desirable to

think about sending in radiation ν and finding ν' as was done before. The variation of ν on either side of ν_o was considered before, since the line had non-zero intensity at points other than ν_o. This non-zero intensity was due to collision or other types of broadening. Here there is no such initial line width. Hence, it is proper to consider an incident radiation ν and calculate the shape of the "line" due to the random velocities of the molecules. Once again the intensity is proportional to the number of absorbers. Using this fact and the Maxwellian distribution, the intensity is written as

$$I \propto \int_{-\infty}^{\infty} \exp(-\tfrac{1}{2}mV_x/kT)dV_x. \qquad [II\text{-}16]$$

In the same way that Equation [II-8] was derived, one may write $\nu - \nu_o = V_x/c$. Combining this with Equation [II-16] and writing the proportionality constant as I_o, the maximum intensity, yields

$$I = I_o \exp[-mc^2(\nu - \nu_o)^2/2kT\ {}_o{}^2]. \qquad [II\text{-}17]$$

A plot of I versus ν is the familiar Gaussian curve. This plot is shown in Figure 10, along with the half-power points and line width.

The line width (Δw) is found from Equation [II-17] and the definition of line width, that definition being that $2(\Delta w)$ equals the distance between the half power points. The actual width of the line is $2(\Delta w)$ but Δw is

often called the line width. To find the half power points from Equation [II-17], make the substitutions $I = \frac{1}{2}I_o$ and $\nu - \nu_o = w$. This immediately gives

$$w = \nu_o/C(2kT\ln 2/m)^{\frac{1}{2}}. \qquad [II-18]$$

In summary of the case of small $\Delta\nu$, one may conclude that the line width Δw varies as $T^{1/2}$. In this experiment low pressures and therefore small $\Delta\nu$ were avoided because errors in pressure measurements were relatively large. These problems are discussed in Chapter III.

Large $\Delta\nu$

Intuitively, it is seen that when $\Delta\nu$ is large the Doppler contribution will be rather small compared to the total width. Hence, in the limit as $\Delta\nu$ gets large, the Doppler contribution to the line can essentially be neglected, and the line shape is given by the Lorentz shape (Equation [II-10]). At first, it is tempting to solve for $\Delta\nu$ from Equation [II-10] in terms of T. However, $\Delta\nu$ is not a variable in that equation but a constant known from the collision process. If one wants to know the temperature dependence of $\Delta\nu$, then that dependence must be found from pressure-broadening theories, taking into consideration nearby spectral lines and other sources of broadening. These sources of broadening will be discussed later.

Intermediate Cases

The temperature dependence of the Doppler effect for intermediate cases for this discussion would be more properly termed "temperature dependence of the Doppler correction." This correction is that quantity which must be summed with the half width between points of steepest slope on the line shape so that the Doppler effect is removed from the line width, $\Delta\nu$. What remains is the derivative of the line shape that would be observed if the Doppler effect were not present. Figure 11 serves to clarify this point.

In Figure 11(A), $2(\delta\nu)'$ is the frequency spacing between the peaks. In Figure 11(B), $2(\delta\nu)$ is the corresponding frequency spacing in a "no-Doppler-effect universe." As was mentioned in Chapter I, there is a relation between $\delta\nu$ and $\Delta\nu$, the quantity sought in the final analysis. (4)

That relationship is expressed as

$$\delta\nu = \frac{\Delta\nu}{\sqrt{3}}\left[1 + \frac{1}{4}(\omega/\Delta\nu)^2 + (f/\Delta\nu)^2\right], \qquad [II\text{-}19]$$

where ω = angular frequency excursion of the klystron due to the applied square wave modulation signal, and
f = angular frequency of modulation.

From Equation [II-19], it is seen that the modulation process affects the half width between points of steepest slope. The importance of this will be seen in the following discussion of the correction that effectively removes the Doppler effect.

In finding this correction, one first finds the points of steepest slope in Equation [II-15] by solving $dI/d\nu = 0$ for ν. The separation of these two frequencies is then compared to the corresponding separation in the derivative of Equation [II-10]. The difference in these two separations is the desired correction that will effectively remove the Doppler effect. Doppler correction curves have been obtained by Parsons and Roberts. (3) Figure 12 illustrates the results of their solution. The straight line is an aid for interpolation and is given specifically for the (8,6) inversion line of ammonia. Each curve has associated with it a normalization factor, B, given by

$$B = mc^2/2kT\nu_o^2. \qquad [II-20]$$

Therefore, a microwave line of frequency ν_o associated with any molecule of mass m in a gas at a particular temperature T has a value of B that can be found directly from Figure 12 or by interpolation between the curves shown. Hence, all that is needed to make the curves apply to a given line of a particular gas is to adjust the temperature scale in accordance with Equation [II-20].

In actual practice, the line-shape derivative will not be the same as the derivative of Equation [II-15]. This is because of the extra width produced by the application of a modulation signal (Equation [II-19]). Figure 13 illustrates the effect by showing an exaggerated case.

The line-shape derivative is shown for the cases of modulation plus Doppler effect, Doppler effect only, and a pure line derivative. The frequency spacing $((\delta\nu)' - \Delta\nu/3^{\frac{1}{2}}) = Z$ is desired as the correction term for compensating the Doppler effect.

Experimentally, one measures $(\delta\nu)''$ shown in Figure 13(A). In order to find Z, given this initial value of $(\delta\nu)''$, one first solves $(\Delta\nu)'$ from Equation [II-19] where $(\delta\nu)$ is replaced by $(\delta\nu)''$ and $\Delta\nu$ by $(\Delta\nu)'$. The value $(\Delta\nu)'$ is the width a spectral line would have if the shape of its derivative was as shown in Figure 13(B). This value of $(\Delta\nu)'$ is then used to find $(\delta\nu)'$ where $(\delta\nu)' = (\Delta\nu)'/3^{\frac{1}{2}}$. Notice there are no terms here due to modulation, since Figure 13(B) assumes no modulation. The desired correction is then $(\delta\nu)' - (\delta\nu) = (\delta\nu)' - \Delta\nu/3^{1/2} = Z$, as shown in Figure 13(C). When this correction is applied to Figure 13(B), both modulation effects and the Doppler effect are compensated for.

The curves in Figure 12 are not experimentally checked; rather, they are applied as corrections. Their validity is assumed for two reasons. First, when these corrections are applied to curves describing line width variations with pressure (at constant temperature), the result is a straight line as predicted by theory. The second argument is that Doppler broadening experimentally agrees with theory

based on the Maxwellian distribution. (1) This experimental confirmation is for frequencies in the visible spectrum.

Wall Broadening

The purpose of finding the wall broadening is so that its effect can be removed from the Doppler-corrected half width. This will leave $\Delta\nu$ versus T as a function of the interaction potential of the colliding molecules only. Finding the nature of this interaction potential is the ultimate goal of the study.

From the kinetic theory of gases the probability, P_A, of a molecule having a collision with a surface of area A in a time interval Δt is

$$P_A = \left(\frac{A}{V}\frac{RT}{\pi M}\right)^{\frac{1}{2}} \Delta t, \qquad [II\text{-}21]$$

where V = volume of the container,
R = universal gas constant,
T = absolute temperature, and
M = molecular weight of the molecule.

Equation [II-21] was derived using the relative velocity between the colliding molecules, which in turn was based on the Maxwellian distribution of velocities.

For the present discussion, the area A is assumed to be inside area of the absorption cell plus the area of all the imaginary spheres concentric, respectively, with each of the molecules in the gas. This area is given by $A = A_1 + 4\pi r^2 n$, where A_1 is the inside area of the cell

and n is the number of molecules in the cell. The diameter, 2r, of the sphere is the distance between the molecules when their interaction potential becomes sufficiently great to interrupt the emission of radiation from the observed molecule.

The probability for one collision is P = 1, and the time required is given by $t = V/A(2\pi M/RT)^{1/2}$. The half width of the line as a result of this finite time between collisions is

$$\Delta\nu = \frac{1}{2\pi} \frac{(A_1 + 4\pi r^2 n)}{V} \left(\frac{RT}{4\pi^3 M}\right)^{\frac{1}{2}} \qquad [II-22]$$

where $A_1 + 4\pi r^2 n$ is substituted for A. The first term in Equation [II-22] is for wall broadening and the second term is for pressure broadening, since n is proportional to the pressure alone at constant temperature.

When the change of A_1/V with temperature is considered, it is seen that this quantity varies in value from room temperature to 50°C by less than .1 per cent. Thus, this temperature dependence may be neglected.

The calculated value for the wall-broadening half-width of ammonia in an X-band waveguide at room temperature is 8.65 kilohertz. When compared to experimental results, this value is found to be several times too small (measured half width is about 38 kilohertz). This is not surprising, since Equation [II-22], from which this value was calculated, was derived from the uncertainty principle ($\Delta E \Delta t \simeq \hbar$).

This "approximately equal to h" is undoubtedly the major source of error. With this in mind, the reasonable way to write the wall broadening half width as a function of temperature is

$$(\Delta\nu)_W = CT^{\frac{1}{2}} \qquad [II-23]$$

where C is an empirical quantity obtained from experimental data. The value of C for a particular temperature is obtained by plotting $\Delta\nu$ versus the pressure, applying the Doppler correction, and extrapolating the curve through the $\Delta\nu$ axis as shown in Figure 14.

Not all ammonia lines will extrapolate to give a "wall-broadening" half width of 38 kilohertz. Several lines extrapolate to larger values. This is explained by the fact that a "line" may be composed of several fine-structure component lines whose envelope constitutes the experimentally observed "line." Figure 15 illustrates such a case. In such cases, it is still proper to use the value of $(\Delta\nu)_W$ = 38 kilohertz, even though the extrapolated value is greater. This is important because it will affect the value of C previously mentioned, and this will in turn affect how the wall-broadening correction will distort the Doppler corrected data.

In a plot of $\Delta\nu$ versus T, after the Doppler correction has been applied, the value $(\Delta\nu)_W = CT^{1/2}$ is simply subtracted from each data point, since Equation [II-22]

verifies the fact that the total width is simply the sum of the wall-broadening width and the pressure-broadening width. It can be observed that $T^{1/2}$ in $(\Delta\nu)_w = CT^{1/2}$ will cause the original plot of $\Delta\nu$ versus T to be distorted as mentioned above instead of merely translating the curve along the $\Delta\nu$ axis. After this correction is applied, what is left is $\Delta\nu$ versus T, due to the effects of the interaction potential between two molecules.

Saturation Broadening

Equation [II-10], giving the line shape, can be written as

$$I = \frac{8\pi^2}{3ch}(n_i - n_j)|\mu_{ij}|^2 \frac{\nu\,\Delta\nu}{(\nu-\nu_o)^2 + (\Delta\nu)^2}, \quad [II-24]$$

where n_i = number of molecules in the lower state,
n_j = number of molecules in the upper state.

Equation [II-24] is independent of the incident radiation, I', if $(n_i - n_j)$ is a constant. This thermodynamic equilibrium between the two states exists as long as I' is relatively small. However, if I becomes appreciable, the $(n_i - n_j)$ no longer is constant but depends on I'. It has been shown that the line shape is unaltered except for the maximum intensity being decreased by a factor depending on I. (8) This in turn increases the half width by a factor independent of T.

In this work, great care was taken to avoid saturation. One must be very careful in order to avoid saturation, since a power flux of about one milliwatt per square centimeter is enough to produce saturation of lines below one megahertz in width. (9)

Nearby Lines

A spectral line lying near another spectral line is distorted appreciably in the frequency region between the two lines. This distortion of the line shape may make the line broader or more narrow at its half-power points. In order to avoid this type of broadening, it is necessary to observe spectral lines that are not near other lines. If this is desired, then one should avoid lines in the inversion spectra of ammonia that have a K value of 1. Such lines have hyperfine structure, owing to the interaction of the hydrogen nuclear spins with the magnetic field produced by electronic motion. These hyperfine-structure components distort the main line and cause it to be altered from what it would be if the hyperfine structure were not present.

Inversion lines of ammonia with a value of $J \leq 7$ also have fine-structure components of appreciable size. These lines are produced by the interaction of the quadrupole moment of the nitrogen nucleus with the electron cloud surrounding the molecule. Since the intensity of the

quadrupole line is approximately proportional to $1/J^2$, these satellite lines may be neglected for lines having a value of $J > 7$.

The frequency spacing between spectral lines and their relative intensities determines the resultant broadening of the spectral lines. Since the frequency spacing between two such lines as a function of temperature is not known, all lines studied in this work were selected so that $J \geq 7$ and $K \neq 1$.

Pressure Broadening

What is desired is a temperature dependence of line widths that reflects the interaction energy between the colliding molecules. The method pursued here will not be to bring in purposely this interaction potential, but will be to find how $\Delta\nu$ varies with the temperature T. It will be seen that the interaction potential naturally finds its way into the mathematical structure of $\Delta\nu$ versus T.

It is useful for later discussions to show first that collisions strong enough to cause an interruption of radiation at microwave frequencies are also strong enough to induce transitions between the ground and excited states. (7) Such a collision is called a diabatic or non-adiabatic collision. Actually, the radiation is not necessarily interrupted in the sense that it is abruptly stopped; rather, it could emerge from the collision with a phase

shift. A phase shift of one radian or larger is usually assumed to be equivalent to a complete interruption of the radiation.

If Δf denotes the average change in frequency of the radiation during a collision, then according to the above criterion the phase shift that occurs when the radiation is effectively completely interrupted is

$$2\pi(\Delta f)t > 1, \qquad [II-25]$$

where t = the duration of the collision.

In an approximate manner, Δf is also given by $h(\Delta f) = w$ where w is the interaction energy between the colliding molecules. But, from Equation [II-25], this can be written as $w\ h/t$. If t is written as R/V, where R is the distance between molecules that produces an appreciable interaction and V is the velocity of the molecule, then it is easily seen that w is greater than $h\nu$ where ν is any microwave frequency. In addition to this, at temperatures used in this study (230°K - 350°K), $kT > h\nu$, so that the translational kinetic energy of the molecule is more than enough to supply the above energy, w. The conclusion is that collisions strong enough to cause an interruption of the radiation, and hence broadening of a spectral line, are also strong enough to induce transitions between the ground and excited states. The utility of these ideas will be seen in the following discussions.

The half width, $\Delta\nu$, of a spectral line due to collisions with other molecules is conveniently expressed as

$$\Delta\nu \propto nv\sigma , \qquad [II-26]$$

where n = number of molecules per unit volume,
v = velocity of the radiating molecule, and
σ = effective cross sectional area.

This is essentially the second term in Equation [II-22]. An elementary theory would hold that σ is a constant for all temperatures. Assuming n is a constant, then the half width as a function of temperature may be written as $\Delta\nu \propto T^{1/2}$. However, in a more refined theory it is also reasonable to expect σ to be a function of the temperature. The following considers that possibility.

First, it is noted that some critical impact parameter, b, of the colliding molecules is equal to r, the effective radius of the perturbing molecule, where $\sigma = \pi r^2$. This assumes the radiator is a point mass. In order to obtain a relation between $\Delta\nu$ and T, assuming σ can vary, it is only necessary to find a relation between b and v. This relationship is obvious since by the above discussion $\Delta\nu$ is related to b, and of course v is proportional to $T^{1/2}$. The desired relationship between b and v is provided by the statement made earlier that collisions effective in broadening are also effective in inducing transitions in the radiating molecule. The effective collision cross section has a radius b such that when impact parameters

are less than b, there is an appreciable probability for a transition to occur. This probability will certainly contain b, since the perturbation, and hence the transition probability, is a function of how close the colliding molecules approach one another. This transition probability will also contain v because again the perturbation, and hence the transition probability, will be a function of how long the radiator stays in the vicinity of the perturbing molecule. This "stay" is a function of v. Hence, the transition probability contains the desired relationship between v and b.

From time-dependent perturbation theory, the transition probability is

$$|C|^2 = \left|\frac{i}{h}\int_{-\infty}^{\infty} V_{jk}\exp(i\omega_{ij}t)dt\right|^2 \qquad [II-27]$$

where j = the set of quantum numbers of the initial state of the radiator,
k = the set of quantum numbers for the final state of the radiator,
ω_{ij} = angular frequency of the transition between the i and j levels,
V_{jk} = matrix element for perturbation energy V, and
C = some constant such that $|C|^2$ gives an "appreciable" probability.

As stated previously, all impact parameters equal to or less than b are equally effective in broadening the line, in that they all serve to interrupt the radiation. If the impact parameters fall in this range, the above transition probability has an appreciable value. It is

convenient to assign all collisions effective in broadening a common value of b for their impact parameters, even though many collisions will have impact parameters smaller than b. This is because all collisions having these smaller impact parameters have the same effectiveness in broadening the line, as do the collisions with impact parameter b. Another reason for using this larger value for b is that there is little or no curvature of the path of the colliding molecules. This is illustrated in Figure 16.

For a first order dipole-dipole interaction, V_{jk} in Equation [II-27] is of the form $\frac{C_1}{r(t)^n} = \frac{C_1}{(b^2 + v^2t^2)^n}$, where the substitution $r(t)^n = b^2 + v^2t^2$ is made from Figure 16. The exact form of C_1 has been found and is given by

$$C_1 = \mu^2 \frac{KK'}{\sqrt{J(J+1)}\ J'(J+1)} (2/3)^{\frac{1}{2}}, \quad [II-28]$$

where the primed and unprimed quantum numbers represent the perturber and radiator, respectively. (2) The permanent dipole moment of the molecule is represented by μ. C_1 can be rewritten as $C_1 = \mu_L \mu_L' (2/3)^{1/2}$ where, for example, μ_L is the projection of the dipole moment along the angular momentum axis of the unprimed molecule. Margenau and Warren obtained Equation [II-28] by finding the root mean square of the matrix for fixed values of J,

K, J', K' and for various values of M and M'. Their result is an intuitively satisfying result, since for a symmetric-top molecule all other projections of the dipole moment average to zero as the molecule rotates. It should be pointed out that the entire dipole moment of ammonia averages to zero over relatively long periods of time, due to the inversion process. However, during a collision it is customary to assume the nitrogen atom is in its equilibrium position. This is reasonable since the duration of a collision is short compared to the period of the inversion process. For these reasons, Margenau and Warren omitted the vibrational part of the wave function in deriving Equation [II-28].

When studying a given spectral line, μ_L is a constant, but μ_L' varies as the radiator associated with μ_L collides with molecules in a wide variety of states. Clearly, μ_L' must be replaced by the average projection of the dipole moment along the angular-momentum axes of all the perturbing molecules. This average is given by

$$\bar{\mu}_L' = \sum_{J',K'} \frac{(2J' + 1)\exp(-E/kT)}{\sum_{J'K'} (2J' + 1)\exp(-E/kT)} \frac{\mu|K'|}{[J'(J' + 1)]^{1/2}} ,$$

where μ = 1.468 for ammonia,
E = energy of rotation, given by Equation [I-4(B)], and
$2J' + 1$ = statistical weighting for M degeneracy.

After solving the problem with a computer, it was found that terminating the sum at J' = 25 obtained sufficient accuracy for 350°K, which was approximately the highest temperature used in this study. The results of these calculations at various temperatures are tabulated in Table II. The values found are slightly higher than those found by Smith and Howard in 1950.

Equation [II-27] may not be written as

$$|C|^2 = \left| \frac{-i(2/3)^{1/2}\bar{\mu}_L' \mu_L}{hb^{n-1}v} \int_{-\infty}^{\infty} \frac{\exp(-iQX)}{(1 + X^2)^{n/2}} dx \right|^2 \qquad [II-30]$$

where the substitutions $X = vt/b$ and $Q = \omega_{ij}b/v$ have been made.

At this point, the desired relationship between b and v is found to be

$$b \propto v^{1/(n-1)}. \qquad [II-31]$$

Since $\Delta\nu \propto n v \sigma$ and $\sigma = 4\pi b^2$ from Equation [II-22], where n is the number of molecules and σ is the surface area of a sphere of radius b surrounding the molecule, $\Delta\nu$ may be immediately written as

$$\Delta\nu \propto n\bar{\mu}_L' \, v^{1-[2/(n-1)]}. \qquad [II-32]$$

The final temperature dependence of the line width is obtained by using $V \propto T^{1/2}$ and has the form

$$\Delta\nu = (\text{const.})\bar{\mu}_L' \, T^{(n-3)/2(n-1)}, \qquad [II-33]$$

assuming the number of molecules per unit volume is fixed

as the temperature varies. Since $\bar{\mu}_L'$ is nearly independent of the temperature, as Table II shows, all one needs to know in order to determine the temperature dependence of the half width is how the interaction potential between the colliding molecules varies with their separation. The constant in Equation [II-33] is determined by experimentally determining $\Delta\nu$ at some constant temperature and by knowing the exact form of the interaction potential. This constant cannot be determined theoretically with any degree of accuracy, since it is not clear what "appreciable" value $|C|^2$ should have.

Another difficulty presents itself when there is more than one interaction potential between the colliding molecules. Let these potentials be given by $V = V_1 + \ldots V_K$ and their matrix elements by $V_{jk} = V_{jk} + \ldots V_{jkj} = C_1/r^n + \ldots C_K/r^m$. The process of finding $\Delta\nu$ as a function of T is approached again by finding the relationship between b and v. Upon substitution of the above potential into Equation [II-27], one finds

$$|C|^2 = \left| \frac{-ib}{hv} \int_{-\infty}^{\infty} \left[\frac{C_1}{b^n(1+x^2)^{n/2}} + \ldots \frac{C_K}{b^m(1+x^2)^{m/2}} \right] \exp(iQX)dx \right|^2, \qquad [II-34]$$

which is the analog of Equation [II-30]. The exact relationship between b and v, and hence between $\Delta\nu$ and T, cannot be determined unless n, ..., m are known. Therefore, it is concluded that it would be very difficult to construct

an equation similar to Equation [II-34] and make it fit an experimentally obtained curve unless there was only one predominant interaction potential, as was the assumption upon which Equation [II-33] was derived.

Equation [II-33] was also derived upon the assumption that n, the number of molecules in the cell, is a constant. Experimentally, this is not a good assumption. As the temperature of the cell is varied, outgassing effects will cause n to vary from values predicted by the ideal gas law. The value of n in the cell may be determined at any time by knowing the pressure, temperature, and volume of the absorption cell at that time, and is given by $n = PV/kT$, from the ideal gas law.

Suppose that initially, n has a value of $n_o = P_oV/kT_o$ and, as the experiment proceeds, n changes. If n is evaluated at some later time and found to be $n = PV/kT$, the number by which $\Delta\nu$ should be multiplied in order that the product represents the half width with a constant n_o molecule is

$$n_o/n = P_oT/PT_o. \qquad [II-35]$$

There is another type of pressure broadening unique to this study. As can be seen from Figure 17, the vapor pressure of mercury increases rapidly at temperatures above room temperature. Collisions of the radiating ammonia molecules with the mercury atoms from the McLeod

gauge will add further width to the line. The need for a McLeod gauge in direct contact with the absorption cell will be explained in Chapter III. To obtain this contribution to the line width, Equation [II-22] is written in a more complete form, taking into consideration the presence of the mercury atoms. That equation is

$$\Delta\nu = (1/2\pi)(A_1V_1 + A_2V_2 + A_3V_3)/4V, \quad [II-36]$$

where V_1 = mean speed of ammonia molecules,
$V_2 = 2^{1/2}V_1$, which is the mean relative speed of the ammonia molecules based on the Maxwellian distribution of velocities,
V_3 = mean relative speed between mercury atoms and ammonia molecules,
A_2 = total surface area of all imaginary spheres surrounding the ammonia molecules, and
A_3 = total surface area of all imaginary spheres surrounding mercury atoms.

Since wall broadening and self broadening have already been discussed, only the third of Equation [II-36] will be considered. It is desirable to predict theoretically this half width as a function of temperature, so that it may be subtracted from experimentally determined line widths at corresponding temperatures. This half width may be written as

$$\Delta\nu_{HG} = \frac{V_3}{2\pi}\frac{4\pi r_3^2 n_3}{4V}, \quad [II-37]$$

where n_3 is the number of mercury atoms within the volume V. The effective radius, r_3, of the mercury atom is the radius it would have if its surface just passed through

the center of an ammonia molecule to which it is adjacent. As Figure 18 shows, this radius is the sum of the radii of the mercury atom and the ammonia molecule. It should be noted that the values for the radii used for both are the radii to the outermost electrons. (5) This relatively small effective radius is probably justified, since the mercury posses no permanent dipole moment. Hence, there would be no first-order interaction between the mercury and the ammonia. Higher-order interactions would only become appreciable just before a collision according to a hard-sphere kinetic theory. For simplicity, this hard-sphere radius is used.

If V_3 is written as the square root of the sum of the squares of the root-mean-square velocities of the ammonia molecule and the mercury atom, and if the number of mercury atoms present is written as PV/kT, the final line width due to the presence of the mercury is

$$(\Delta\nu)_{HG} = r_3^2 \left(\frac{2N_o}{kM}\right)^{1/2} \frac{P}{T^{1/2}} , \qquad [II-38]$$

where N_o = Avogadro's number,
k = Boltzmann's constant,
P = partial pressure of mercury, and
$\frac{1}{M} = \frac{1}{M_1} + \frac{1}{M_2}$ (M_1 is the molecular weight of ammonia and M_2 is the atomic weight of mercury.)

CHAPTER BIBLIOGRAPHY

1. Loeb, Leonard B., The Kinetic Theory of Gases, New York, Dover Publications, Inc., 1961, 113.

2. Margenau, Henry and Warren, Dana T., "Long Range Interaction Between Dipole Molecules," Physical Review, LI (May, 1937), 748-753.

3. Parsons, Ralph W., and Roberts, James A., "The Doppler Contribution to Microwave Line Widths," Journal of Molecular Spectroscopy, XVIII (December, 1965), 412-417.

4. Rinehart, E. A., Kleen, R. H., and Lin, C. C., "Measurement of the Widths of Microwave Spectral Lines," Journal of Molecular Spectroscopy V, (December, 1960), 458-473.

5. Roberts, James A., "Studies of Line Width of Microwave Spectra of Symmetric Top Molecules," Dissertation Abstracts, 2649-B, (1967).

6. Schiff, Leonard I., Quantum Mechanics, New York, McGraw-Hill Book Co., 1968, 413-414.

7. Townes, C. H., and Schawlow, A. L., Microwave Spectroscopy, New York, McGraw-Hill Book Co., 1955, 351.

8. _____, Microwave Spectroscopy, New York, McGraw-Hill Book Co., 1955, 373.

9. Townes, C. H., "The Ammonia Spectrum and Line Shapes Near 1.25-cm Wave-Length," Physical Review, LXX (November, 1946), 665-671.

CHAPTER III

EXPERIMENTAL TECHNIQUES AND RESULTS

The placement of the absorption cell and the McLeod gauge is as shown in Figure 19. Owing to the physical dimensions of a McLeod gauge, it is necessary to make the insulated enclosure rather elongated. The presence of the McLeod gauge introduces new problems of uniform temperature control. To overcome this problem, the heating elements were divided into two groups, an upper group and a lower group, with each group controlled by a separate Variac. A plot of the Variac voltage for the upper group versus the voltage for the lower group was experimentally prepared such that the plot represented equilibrium temperatures.

For temperatures below room temperature, compressed air blown through a coil immersed in liquid nitrogen was used for cooling. Attempts were made to obtain several different equilibrium temperatures by regulating the two valves shown. This method was prohibitively difficult, so the following procedure was adopted. The valves were regulated so that the top portion of the insulated enclosure becomes colder than the bottom portion. When the bottom section reached a desired temperature, which was monitored

by a thermopile, the flow of cold air was shut off to both inlets. Because of the glass window in the upper section, this section warmed faster than the lower section. The temperature of this upper section was also monitored by a thermopile, and when that temperature became equal to the lower temperature, measurement of line width, pressure, and temperature measurements were quickly made. An equilibrium temperature could be maintained for about five minutes by opening the cold-air valve to the top section for short intervals of time. Surprisingly, consistent line widths at a given temperature were obtained. (The frequency of the klystron was swept through approximately ten times and ten line width measurements were made.) It was felt that perhaps at these lower temperatures the ammonia would not come to equilibrium quickly and, hence, the pressure would vary as the line width was measured, but apparently such was not the case. Data were taken so quickly below room temperature that it is very doubtful that the mercury vapor reached an equilibrium pressure. Fortunately, the vapor pressure of mercury below room temperature is negligible and this correction to the line width, as was discussed in Chapter II, can be neglected.

The desiccator shown in Figure 19 was found to be necessary since water vapor in the air froze in the lines

and finally blocked them completely. The liquid oxygen trap was also found to be necessary if sharp temperature gradients were to be avoided. Without the trap, oxygen from the air stream is liquified and comes out in spurts, striking the adsorption cell and the McLeod gauge, causing the liquid oxygen to fall to the bottom of a metal container, where it boils as a result of heat absorbed from the surrounding air at room temperature.

Some of the major problems in this study were encountered in trying to obtain a good vacuum seal at all temperatures used. Flexing of joints in the vacuum system as the temperature changed was a source of trouble. The joints used were the conventional ball and socket joint of Pyrex. Sealing with ordinary black wax resulted in leaks at both high and low temperatures, due to the wax melting or cracking. The method of sealing finally utilized was to first seal with black wax and then run a bead of Torr Seal (manufactured by Varian Associates) around the joint. Since this glue becomes quite brittle even at room temperature, it was felt that another layer of a softer, more flexible sealant should cover the Torr Seal, just in case changes in temperature produced tiny cracks in it. The material chosed for this was Silastic (a product of Dow Corning). The substance produces an excellent seal, will burn before it melts, and is still somewhat flexible just

above the temperature of liquid nitrogen. The only undesirable feature of Silastic is that it absorbs large quantities of gas. After a good vacuum is obtained, relatively large amounts of outgassing will be observed if Silastic is in contact with the system. Even after several days of hard pumping, outgassing from the Silastic will cause the pressure to rise at the rate of approximately three microns per hour. This is undesirable if the outgassing is releasing anything except the gas to be studied, ammonia in this case. However, if the system is previously saturated with ammonia, then it is primarily ammonia that will be released. During a period of five or six minutes, the time ordinarily required for a data run at a given temperature and pressure, the increase in pressure of ammonia due to the outgassing will be negligible. Also since the cell, and hence the Silastic, is previously saturated with ammonia, there is no appreciable foreign gas broadening due to air being outgassed.

In spite of these precautions in sealing, leaks habitually occurred at approximately -35°C. This was not particularly alarming, other than the nuisance of resealing, since only 4°C lower would result in freezing the mercury in the McLeod gauge.

Due to the absorption of large quantities of ammonia onto the aluminum absorption cell walls and the slow rate

at which equilibrium was approached, it was necessary to wait at least one hour after the cell had received a new dose of ammonia or after a new temperature had been reached. With the isolation valve closed in order to prevent a thermal gradient between molecules in the manifold and molecules in the absorption cell, it was observed that at least one hour must pass before the pressure ceases to change. From observations, this statement seems to hold more for temperatures above room temperature than for those below room temperature.

At least one hour per data point is required; however, because of adjustments to be made, such as voltage adjustments to heating elements, removal of standing waves by tuning, and voltage adjustments to the klystron, the time required per data point is closer to two hours. To obtain a satisfactory number of data points, it is necessary to run the equipment continuously for about twenty-four hours. It is important that all data points that are to be displayed on the same graph be taken in this fashion instead of piecemeal. By continuously running the equipment, the same set of frequency markers is obtained for each data point. If a few points were run, the equipment turned off, and the process repeated the next day, it is doubtful that exactly the same set of frequency markers would be displayed. It is extremely important that each data

point be taken with respect to the same set of frequency markers. It is not even critical that the exact frequency between the markers be known, since it is the relative frequency spacing of the lines that is important. However, it is of utmost importance that the frequency spacing of the markers remain constant for all data points, and it was for this reason that data runs were done continuously instead of piecemeal.

As was mentioned previously, for each data point (taken at a specific temperature and pressure), approximately ten traces of the line derivative were obtained on the chart recorder along with frequency markers. Using the same corresponding frequency markers, each derivative was measured for the frequency spacing between points of steepest slope. For each data point, the average of this frequency between points of steepest slope was found. This average, along with the voltage from the thermopile, H, and h from the McLeod gauge was fed into the computer. The computer then tabulated the corresponding temperatures, corrected pressure, uncorrected pressure, projection of the dipole moment, and the frequency spacing between points of the steepest slope after the modulation broadening effect was removed. The Doppler correction is now obtained graphically from Figure 12, and the vapor pressure of mercury is found from Figure 17. The computer

is reprogrammed and fed this new information. The final output is the line width with wall broadening, Doppler effect, and broadening due to collisions with mercury atoms removed.

The data obtained from the (8,6) inversion line of ammonia are displayed in Figures 20 and 21. They represent two different runs. The values of $\Delta\nu$ shown are effectively for a constant number of molecules in the cell such that the pressure is 21.929 microns at 300.01°K. Also, $\Delta\nu$ is corrected so that the change of the dipole moment projection on the angular momentum axis is removed. In other words, the experimental plot of $\Delta\nu$ versus T is due only to the interaction potential and nothing else. Notice that the curve in Figure 21 reproduces the curve in Figure 20 quite well in its main features.

The dip in the curve with a minimum at approximately 322°K is not clearly shown to be there by the data points given in Figures 20 and 21. However, there is strong evidence of its existence when points of nearly the same temperature are observed in the neighborhood of the dip. Wide separation of half widths at approximately equal temperatures indicates a very steep slope.

The dashed curve shown in Figure 20 is the curve that seems to be a best fit if all resonances and dips are removed from the experimental curve. This curve is for n

greater than any n given in Table I. It seems that an exponential-type interaction might be needed to explain the steepness of the curve. Figure 22 shows what the curve is believed to look like at both higher and lower temperatures after extrapolation. This is supported in part by two data points obtained by Smith and Howard. (1) Their two points fell approximately on the curve given by n = 3, which is to be expected if only a dipole-dipole interaction exists. For n = 3, the plot of $\Delta\nu$ versus T is a straight line, assuming the number of molecules in the cell to be a constant.

It is not at all clear exactly what the interaction potential is from the experimental curve; however, it is clear that if the variation of $\Delta\nu$ with T as is shown is due only to the interaction potential, then that potential is considerably more complex in form than $1/r^n$. In fact, it need not be some peculiar interaction potential that explains the apparent anomalies in the curve. These anomalies could be explained by temperature dependent factors somewhat analogous to the dipole moment projection factor.

Future studies on this subject could lead to valuable new information concerning the ammonia molecule. It is recommended that a wide variety of spectral lines of ammonia be observed to determine if the resonances are a property of ammonia in general or just the (8,6) line.

These future studies should be done with a broader temperature range. This would necessitate the development of a better sealing arrangement at joints, and also the development of a modified McLeod gauge. It is suggested that the mercury be replaced by some liquid that has a lower freezing point than mercury, as well as a lower vapor pressure. This change would not only allow lower temperatures to be reached, but would also minimize any errors that might be present in the method used for foreign gas broadening corrections. Using a McLeod gauge having a larger ratio of V to V' would permit the use of lower density liquids, without making the capillary tubes excessively long.

Foreign-gas broadening experiments are not recommended because little is presently known about the adsorption rates of different gases onto aluminum (the absorption cell is made of aluminum) at various temperatures. Although in such an experiment the pressure could be measured directly as it is in this one, it would be impossible to tell what fraction of the total pressure should be attributed to the foreign gas.

CHAPTER BIBLIOGRAPHY

1. Smith, W. V., and Howard, R. R., "Temperature Dependence of Microwave Line Width," Physical Review, LXXVII (March, 1950), 840-841.

APPENDIX I

TEMPERATURE CORRECTIONS ON MCLEOD GAUGE READINGS

As was mentioned in the section on pressure broadening in Chapter II, outgassing effects cause the pressure in the absorption cell to deviate from that predicted by the ideal gas law. Thus it is necessary to measure the pressure directly each time the line width and the corresponding temperature are measured. The presence of the mercury in the McLeod gauge introduces two new problems, one of thich was discussed in Chapter II. That problem was the broadening of the spectral line due to collisions of the ammonia radiators with the mercury atoms. The other problem is that corrections must be made to the pressure readings since temperature changes affect the relative volumes of the gauge, as well as changing the density of the mercury. To investigate these problems, it is necessary to study the effects of temperature on the fundamental equations associated with a McLeod gauge.

In investigating these problems, the main objective is to derive an equation that gives the correction that must be applied to a McLeod gauge reading for variations in temperature. Instead of deriving the equation in terms of the various volumes and other parameters associated with

the particular McLeod gauge used, it is desired to express the equation in terms of a calibration constant. This calibration constant is obtained by calibrating the gauge against another McLeod gauge whose readings are known to be accurate. This process of calibration was chosen in order to avoid the tedious process of measuring the volume of the gauge.

As will be shown in the following discussion, the pressure in microns of the mercury of the calibrated gauge will be given as $P_1 = C'Hh$ at room temperature. H and h are shown in Figure 23 and are measured directly in centimeters with a cathetometer. C' is the calibration constant obtained when the test gauge is calibrated against the standard gauge.

In Figure 23, V is the combined volume of the bulb and the closed capillary tube above the dotted line. The volume $V' = AH$ is the volume of the compressed gas in the closed capillary tube. From Figure 23, it is seen that $P_1V = P_1'V'$, where P_1 is the partial pressure of the NH_3. P_1' will be approximately the total pressure of the compressed gas, since mercury vapor is a condensable vapor. Also, it is seen that $P_1' = P_1 + P_2 + \rho gh$, where ρ is the density of the mercury and P_2 is the partial pressure of the mercury vapor. This last equation is true only if the system whose pressure is to be measured is large in volume

compared to that of the McLeod gauge. This volume relationship is generally true and is true in this experiment since the manifold and absorption cell volume, V, is several hundred times larger than the volume of the McLeod gauge test volume.

Eliminating P_1' from these last equations yields $P_1 = (V'\varrho gh + P_2V')/(V - V')$, which may be written as $P_1 = (V'\varrho gh + P_2V')/V$, since $V' \ll V$. Also, since $V' = AH$, the pressure may be written as

$$P_1 = CHh + CP_2H/\varrho g, \qquad [1]$$

where $C = A\varrho g/V$.

As the temperature varies, A, ϱ, and V vary. Let

A_o = initial cross sectional area of the capillary tube at room temperature,
a = linear coefficient of expansion of the gauge (Pyrex),
ϱ_o = initial density of mercury at room temperature,
D = change in density of mercury per degree centigrade, and
V_o = initial volume of McLeod gauge above dotted line in Figure 23.

With variations in temperature, T, Equation [1] becomes

$$P_1 = \frac{(A_o + 2A_oa\Delta T)(\varrho_o + D\Delta T)}{V_o + 3aV_o\Delta T} + \frac{CP_2H}{g(\varrho_o + D\Delta T)}, \qquad [2]$$

where the temperature dependence of P_2 is not explicitly written in.

After some algebraic manipulation, P_1 may finally be written as

$$P_1 = \frac{CHh[1 + E\Delta T/\rho_o + 2a(\Delta T)^2 D/\rho_o]}{(1 + 3a\Delta T)} + \frac{CP_2H}{g(\rho_o + D\Delta T)} \qquad [3(A)]$$

$$E = (D + 2a\rho_o) \qquad [3(B)]$$

$$C = A_o\rho_o g/V_o \qquad [3(C)]$$

It is desirable to express the pressure in microns of mercury instead of force per unit area, as Equation [3(A)] does. This is especially convenient since the calibration constant, C', for the gauge used is such that $P_1 = C'Hh$ yields the pressure in microns, with H and h being measured in centimeters. Notice that this last pressure equation is proportional to Equation [1] if the vapor pressure of the mercury is neglected, as is usually the case at room temperature. Since it is desirable to avoid physical measurements of the quantities in C, it is desired to express C in terms of C', which is an explicitly known constant from a calibration of the McLeod gauge.

Since C'Hh is the height in microns, it is easily seen that the pressure in dynes/cm^2 is given by

$$P_1 = (C'Hh) \times 10^{-10} \rho_o g, \qquad [4]$$

where the quantity in brackets gives the height of mercury in centimeters.

After comparing Equations [1] and [4] and neglecting the second term of Equation [1], it is seen that C is given by $C'\rho_o g \times 10^{-10}$. Thus, if the pressure in microns

is given by $P_1 = C'Hh$, conversion to dynes/cm^2 is achieved by multiplying by $\rho_o g \times 10^{-10}$, as Equation [4] shows. Conversely, if given the pressure in dynes/cm^2, all that is needed to convert back to microns is to divide by $\rho_o g \times 10^{-10}$. Equation [3(A)] may now be expressed in microns by inserting the quantity just found for C and dividing by $\rho_o g \times 10^{-10}$. But this is equivalent to just replacing C by C'; hence, the temperature-corrected pressure is now

$$\frac{C'Hh[1 + E\Delta T/\rho_o + 2a(\Delta T)^2 D/\rho_o]}{(1 + 3a\Delta T)} + \frac{C'P_2H}{g(\rho_o + D\Delta T)} . \qquad [5]$$

If the pressure, P_2, is known in microns, it will be necessary to replace it by $P_2'\rho_o g \times 10^{-10}$, where P_2' is the pressure in microns of mercury of the mercury vapor. In this experiment, H seldom exceeded 10 centimeters so the second term of Equation [5] is quite negligible when compared to the first because of the factor 10^{-10}.

In its final form, the equation giving the pressure in microns of mercury is

$$P_1 = \frac{C'Hh[1 + E\Delta T/\rho_o + 2a(\Delta T)^2 D/\rho_o]}{1 + 3a\Delta T} . \qquad [6]$$

Table III shows some typical uncorrected and corrected pressures calculated from this formula at various temperatures.

APPENDIX II

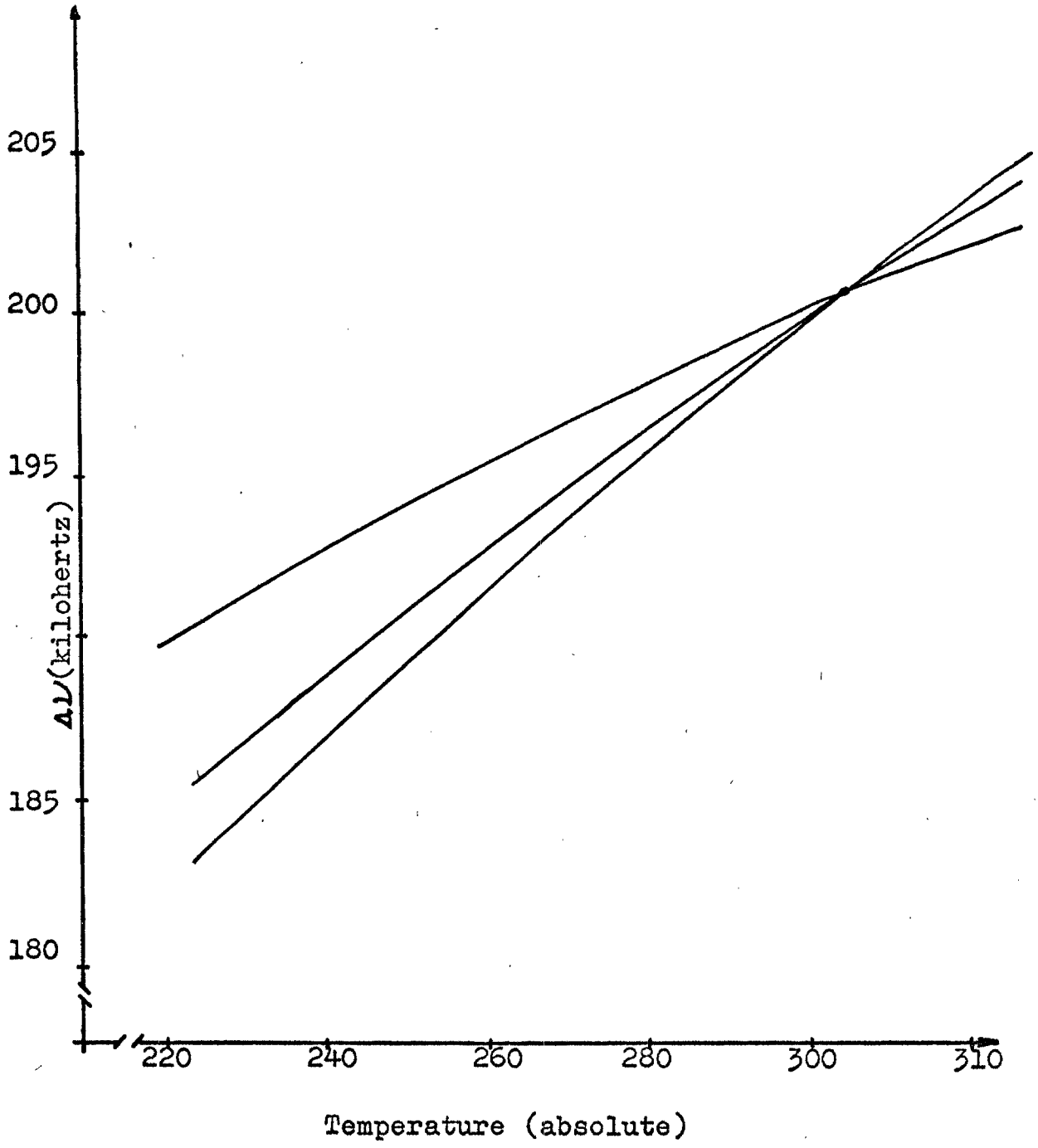

Figure 1

Line width ($\Delta\nu$) versus temperature for (1) $\Delta\nu \propto T^{0.3}$, (2) $\Delta\nu \propto T^{1/4}$, and (3) $\Delta\nu \propto T^{1/6}$. To facilitate comparison, $\Delta\nu$ is arbitrarily assigned a value of 200 kilohertz at 301° K.

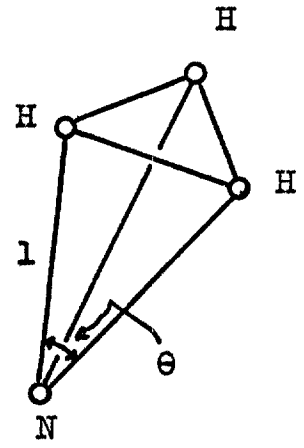

Fig. 2 --- Configuration of the ammonia molecule.

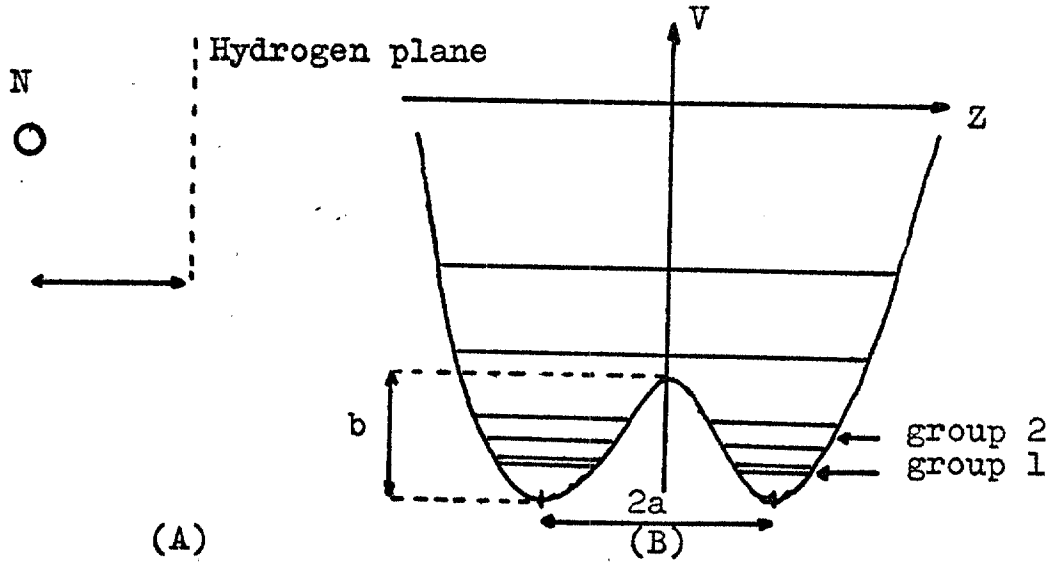

Fig. 3 -- (A) The distance a is the equilibrium distance of the nitrogen atom from the hydrogen plane. The nitrogen atom vibrates along a line perpendicular to the hydrogen plane.

(B) Potential as seen by the nitrogen atom as a function of Z along with the first few energy levels.

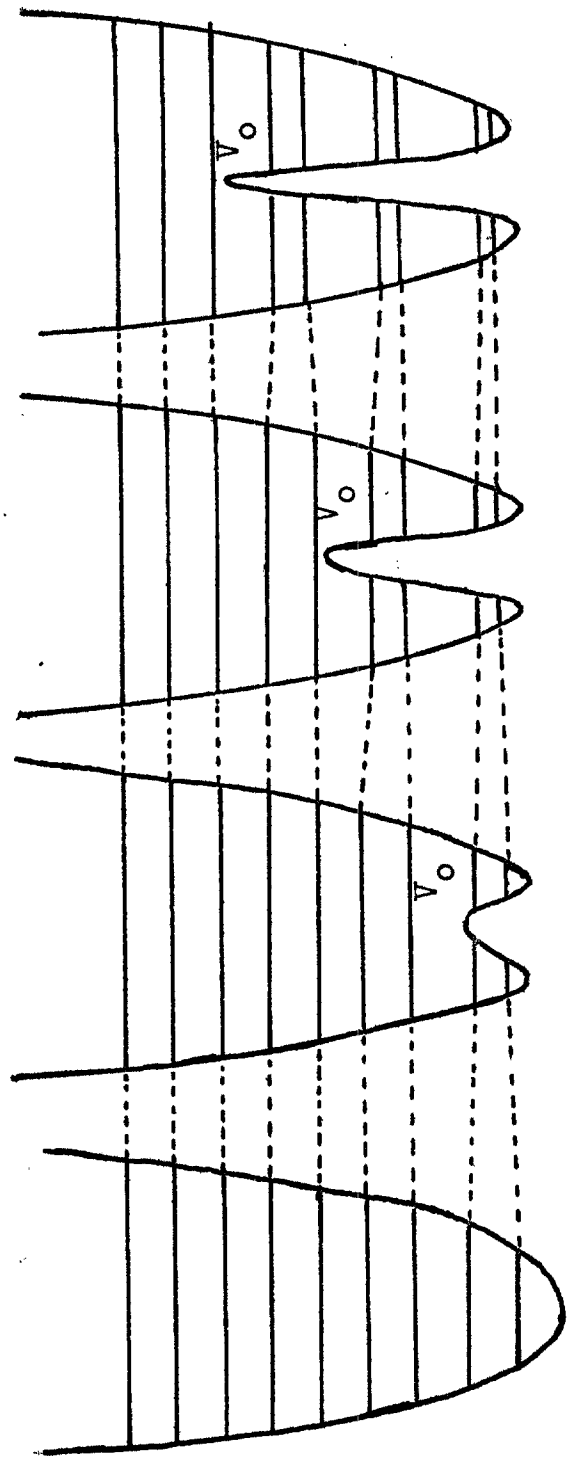

Fig. 4 -- Energy levels of the double oscillator as a function of the barrier height.

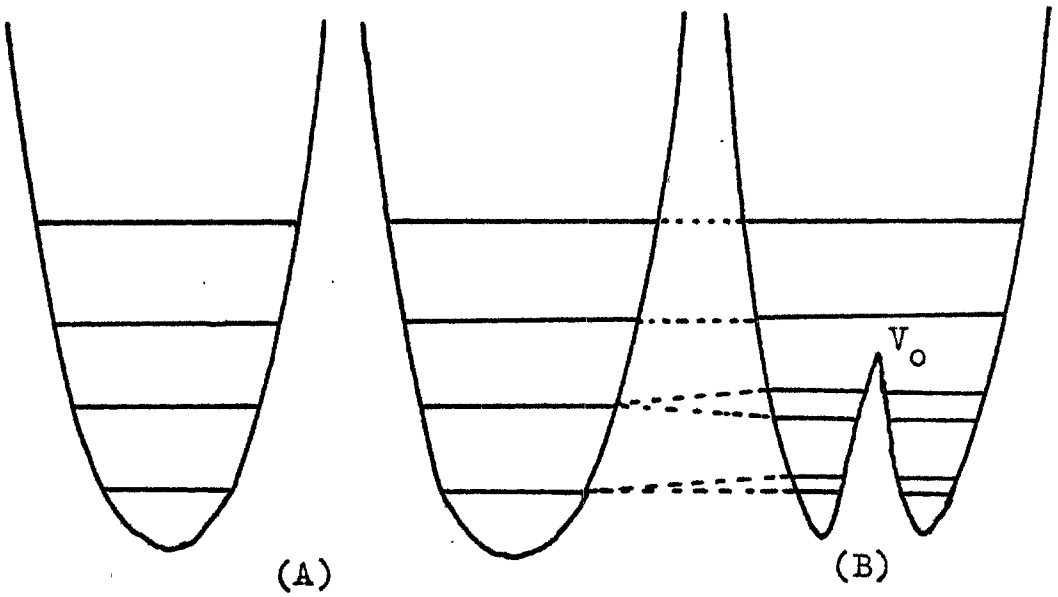

Fig. 5 -- (A) Two separate harmonic-oscillator potentials (infinite barrier V_o) along with energy levels.
(B) Double oscillator with finite barrier V_o along with the split energy levels.

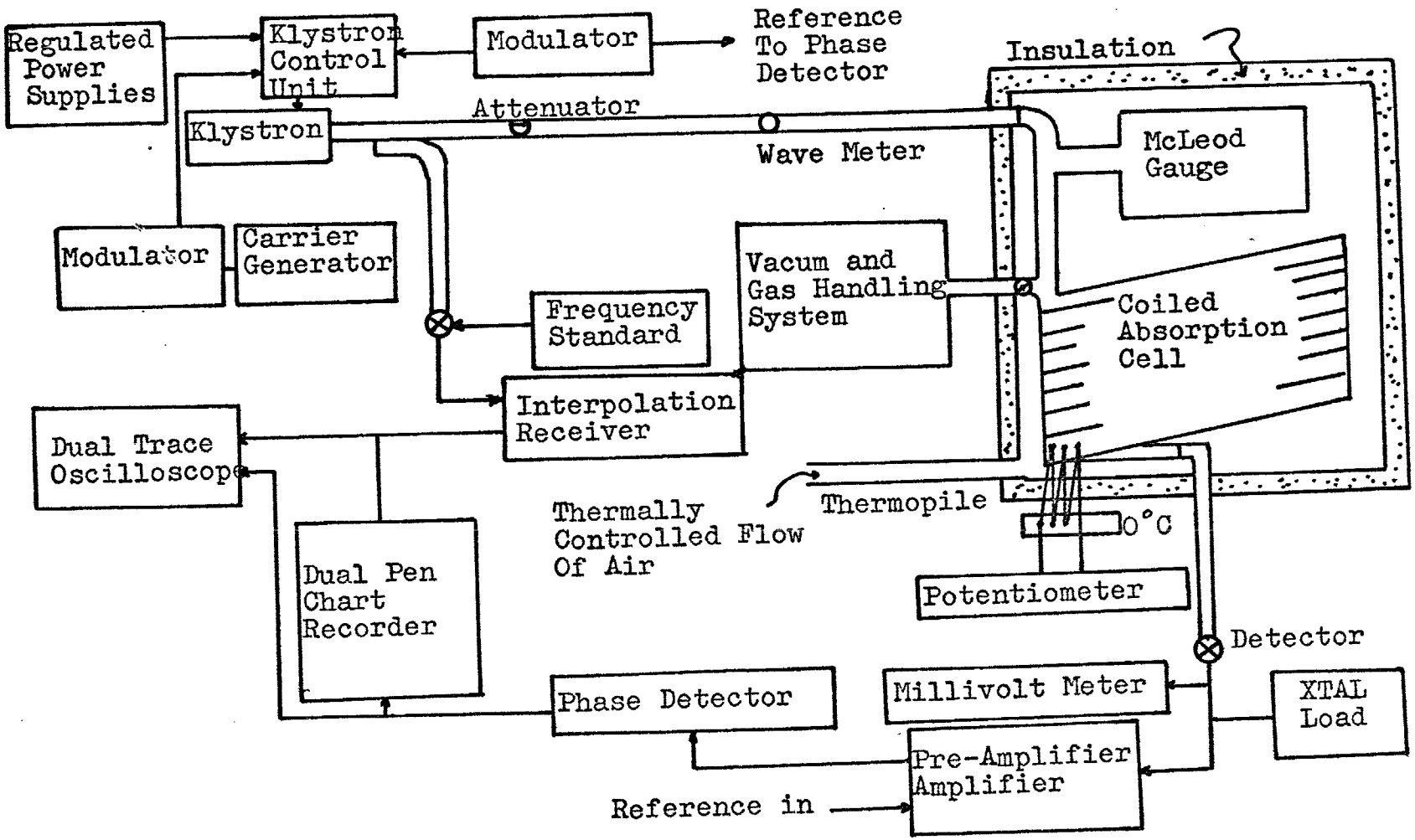

Fig. 6 -- Block diagram of microwave spectrograph used in temperature study.

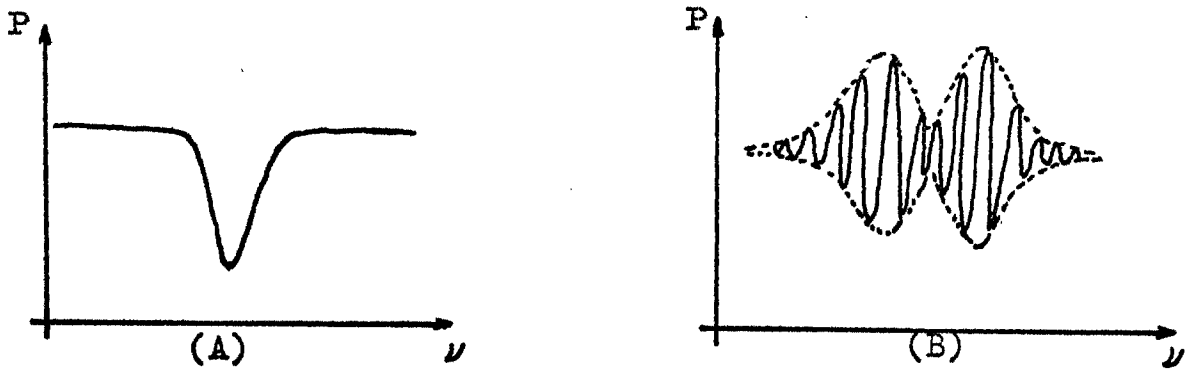

Fig. 7 -- (A) Power "observed by detector-amplifier system with an unmodulated sweep on repeller.
(B) Power with modulated sweep.

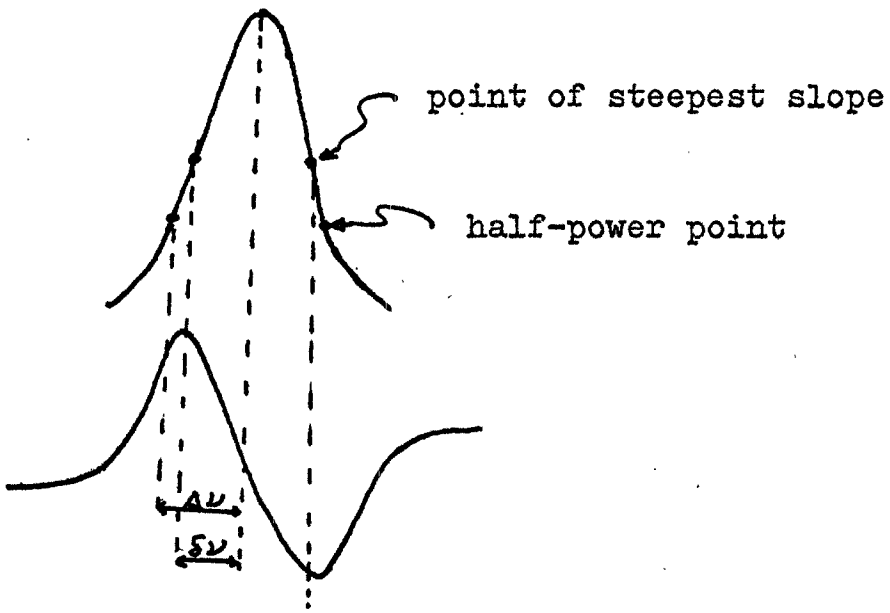

Fig. 8 -- Line shape and its derivative.

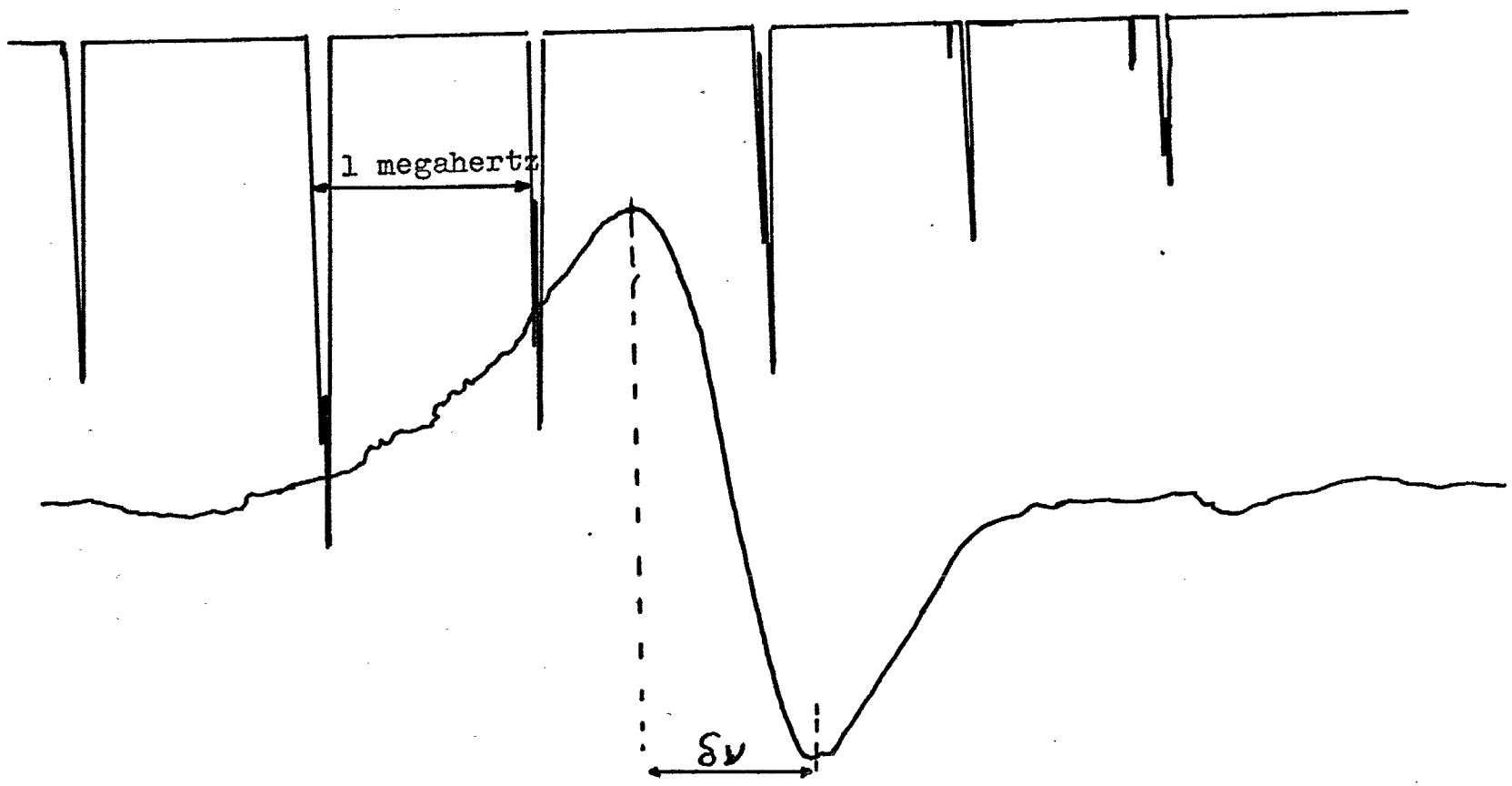

Fig. 9 -- A typical display on the dual-pen chart recorder showing both the line-shape derivative and frequency markers.

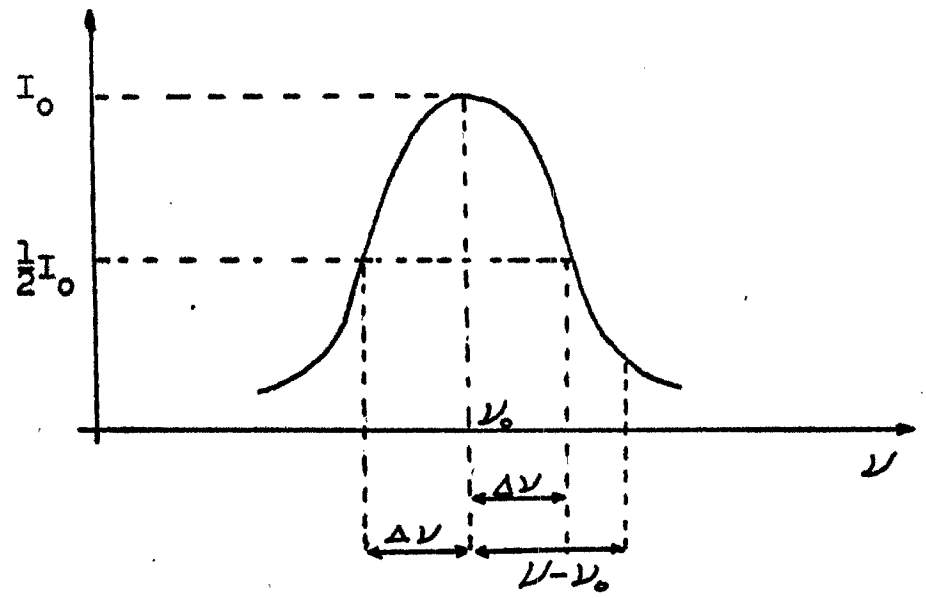

Fig. 10 -- Pure Doppler line shape.

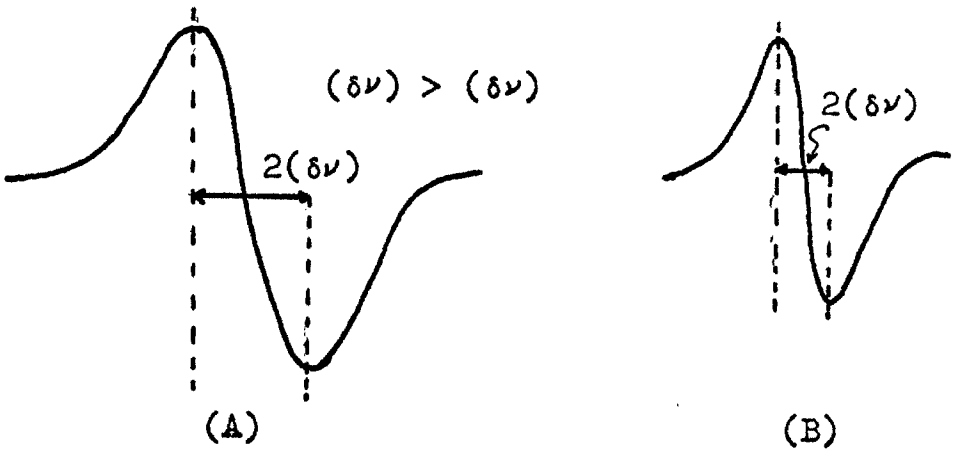

Fig. 11 -- (A) Derivative of line shape that includes Doppler effect.
(B) Derivative of line shape if Doppler effect is not present.

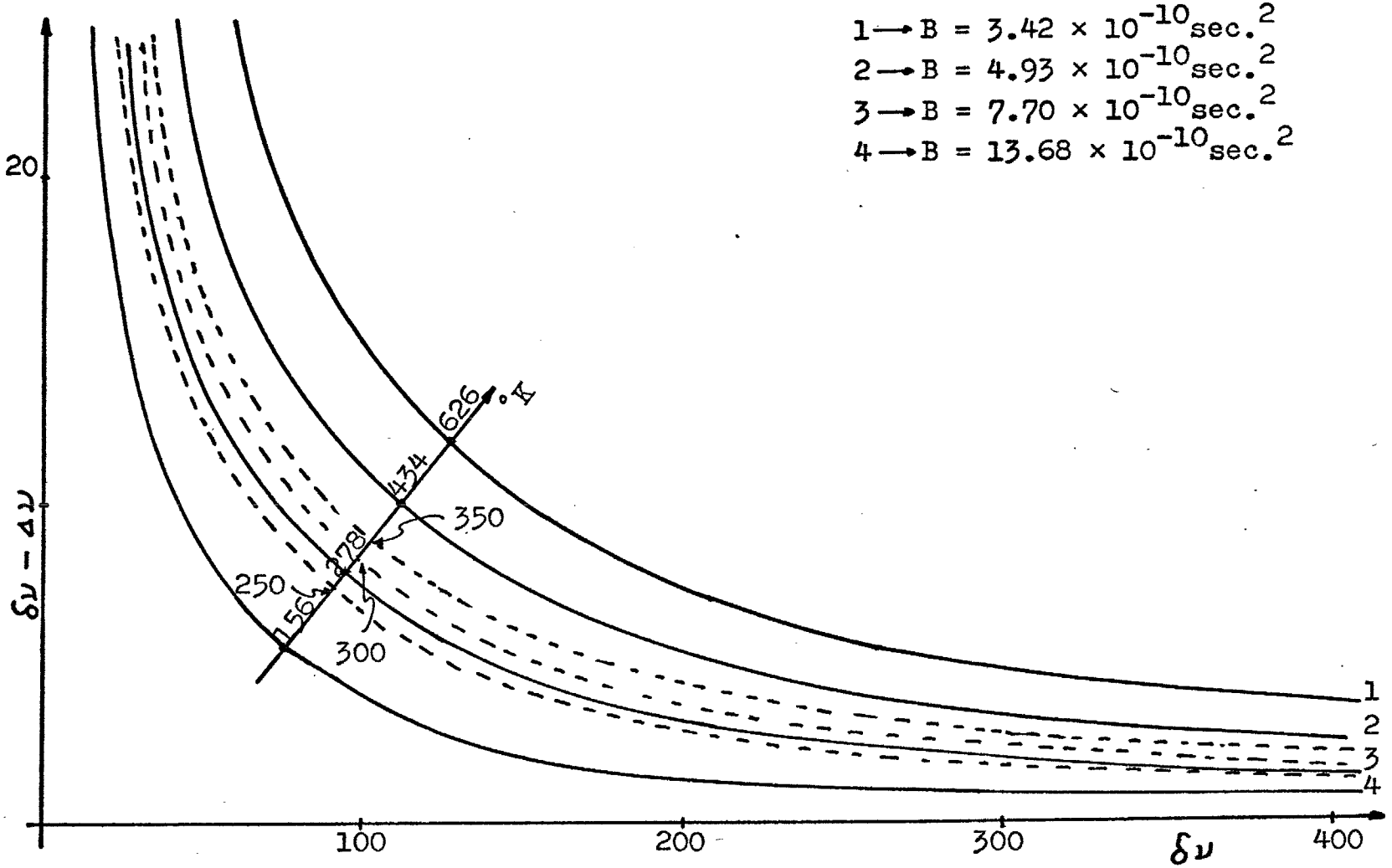

Fig. 12 -- Doppler correction for (8,6) inversion line of ammonia.

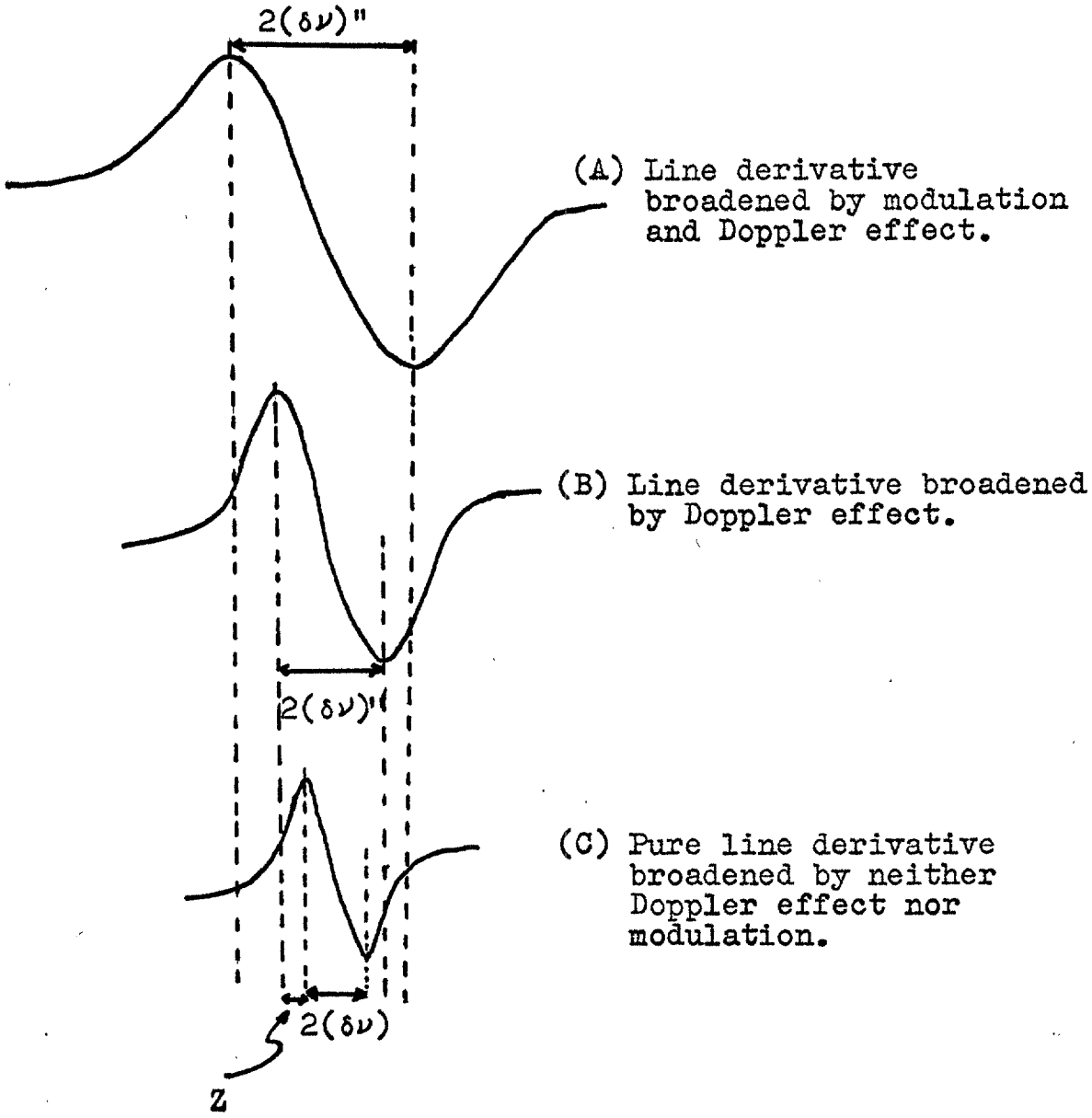

Fig. 13 -- Comparison of width between points of steepest slope to show effect of the modulation and the Doppler effect.

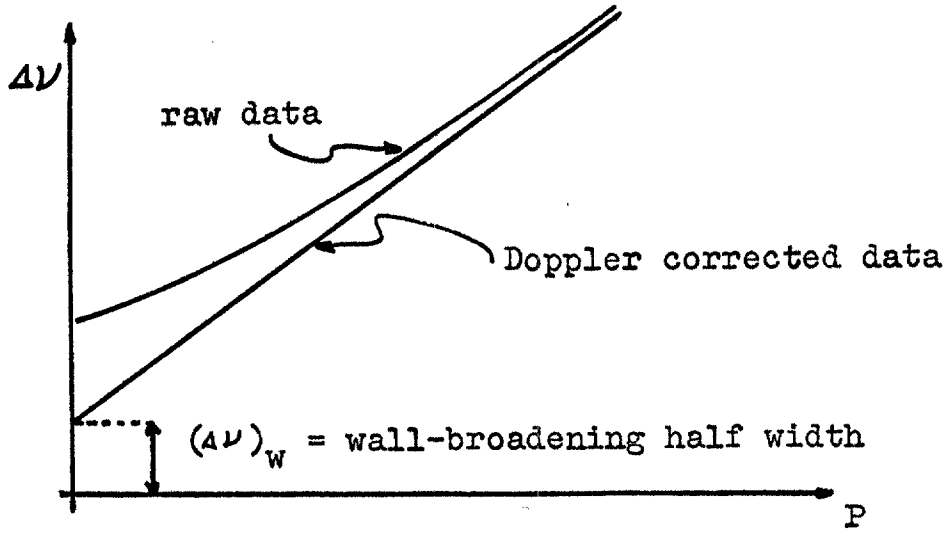

Fig. 14 -- Extrapolation for finding wall broadening.

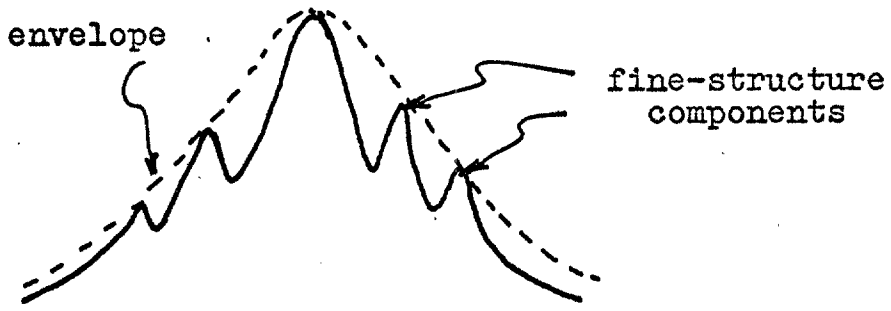

Fig. 15 -- Fine-structure components of a "line" and the resulting envelope.

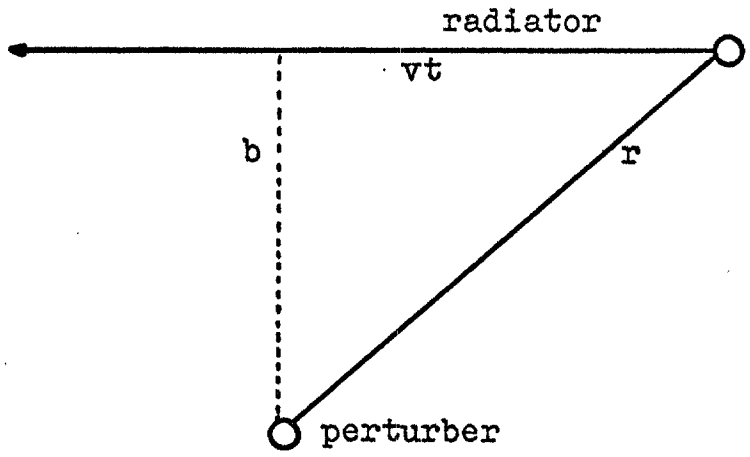

Fig. 16 -- Collision involving no curvature of path.

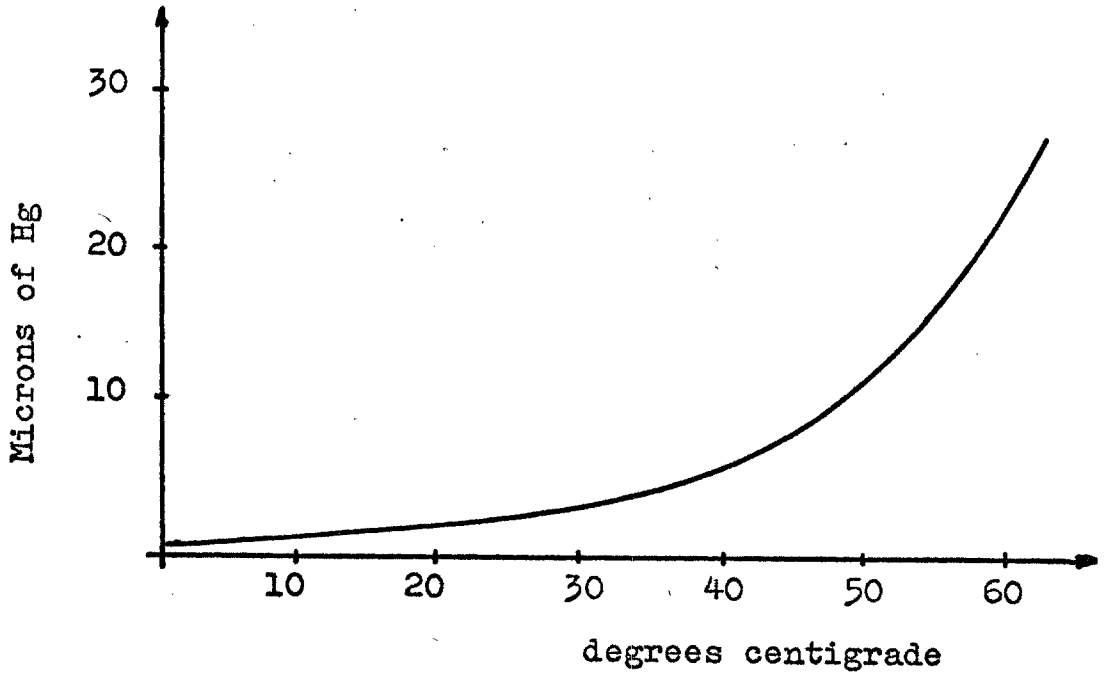

Fig. 17 -- Vapor pressure of mercury as a function of temperature.

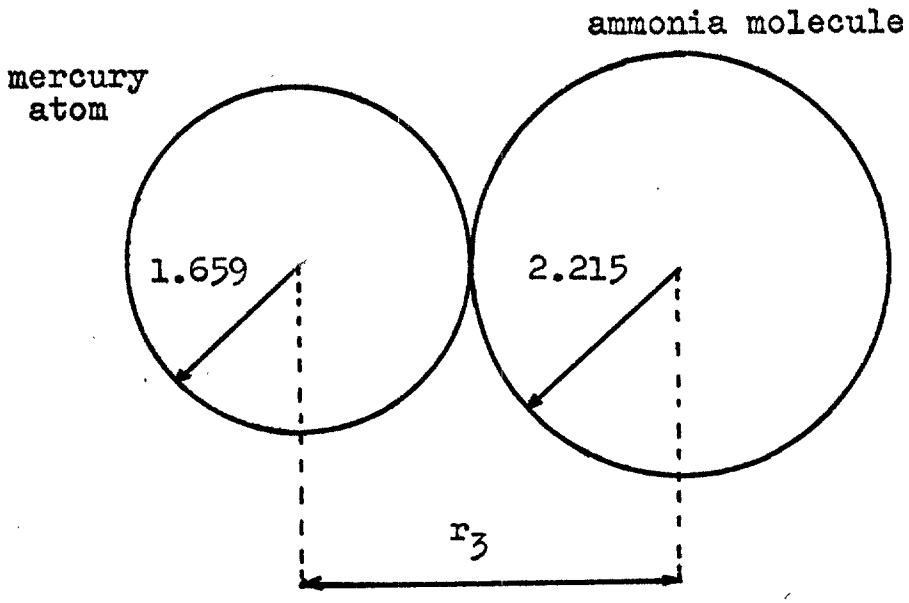

Fig. 18 -- Effective radius, r_3, of mercury atoms when colliding with ammonia molecules. All radii are given in angstroms.

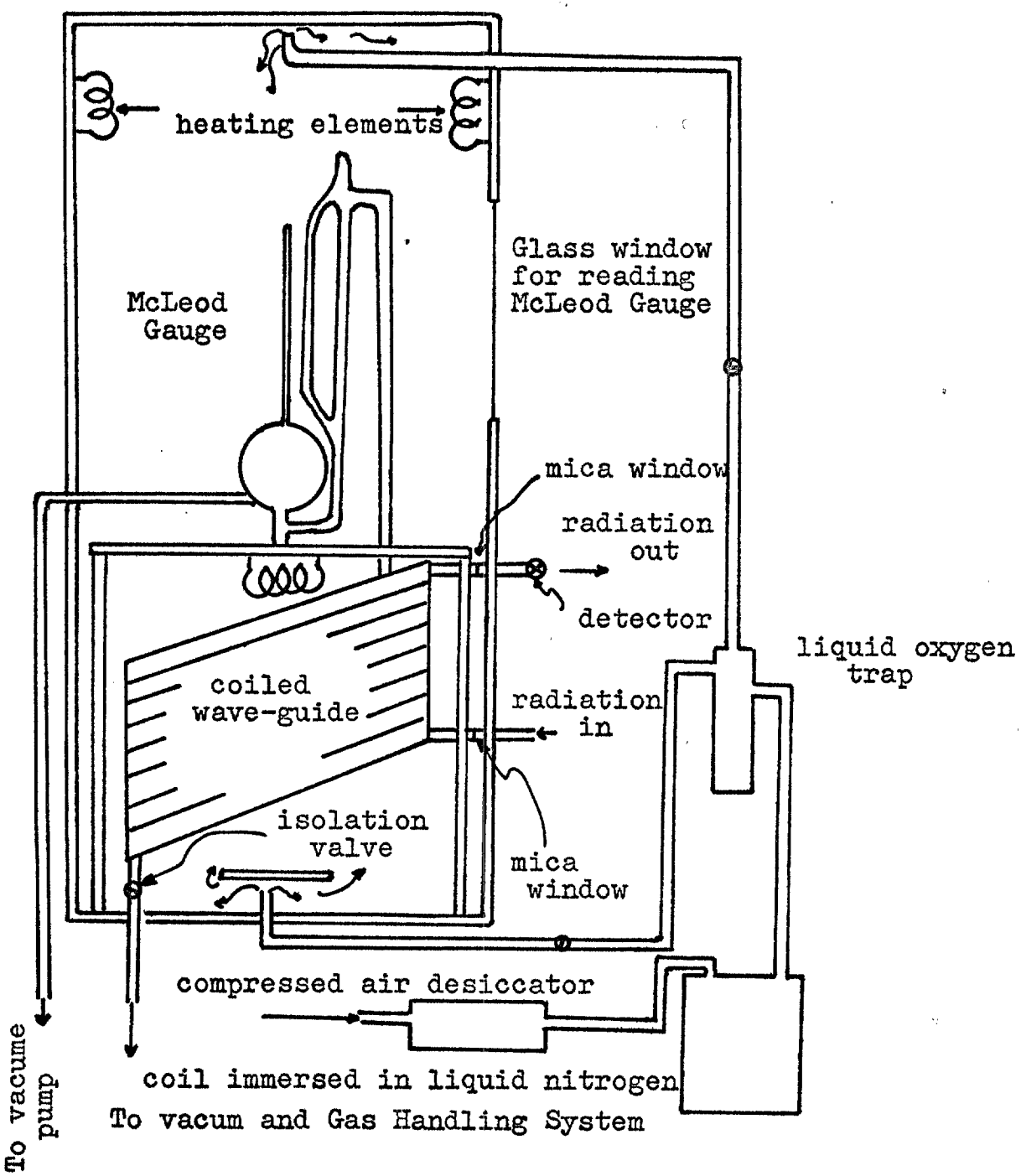

Fig. 19 -- Insulated absorption cell with support equipment for regualtion of temperature. Notice detector is outside the enclosure so as to minimize temperature effects on the crystal.

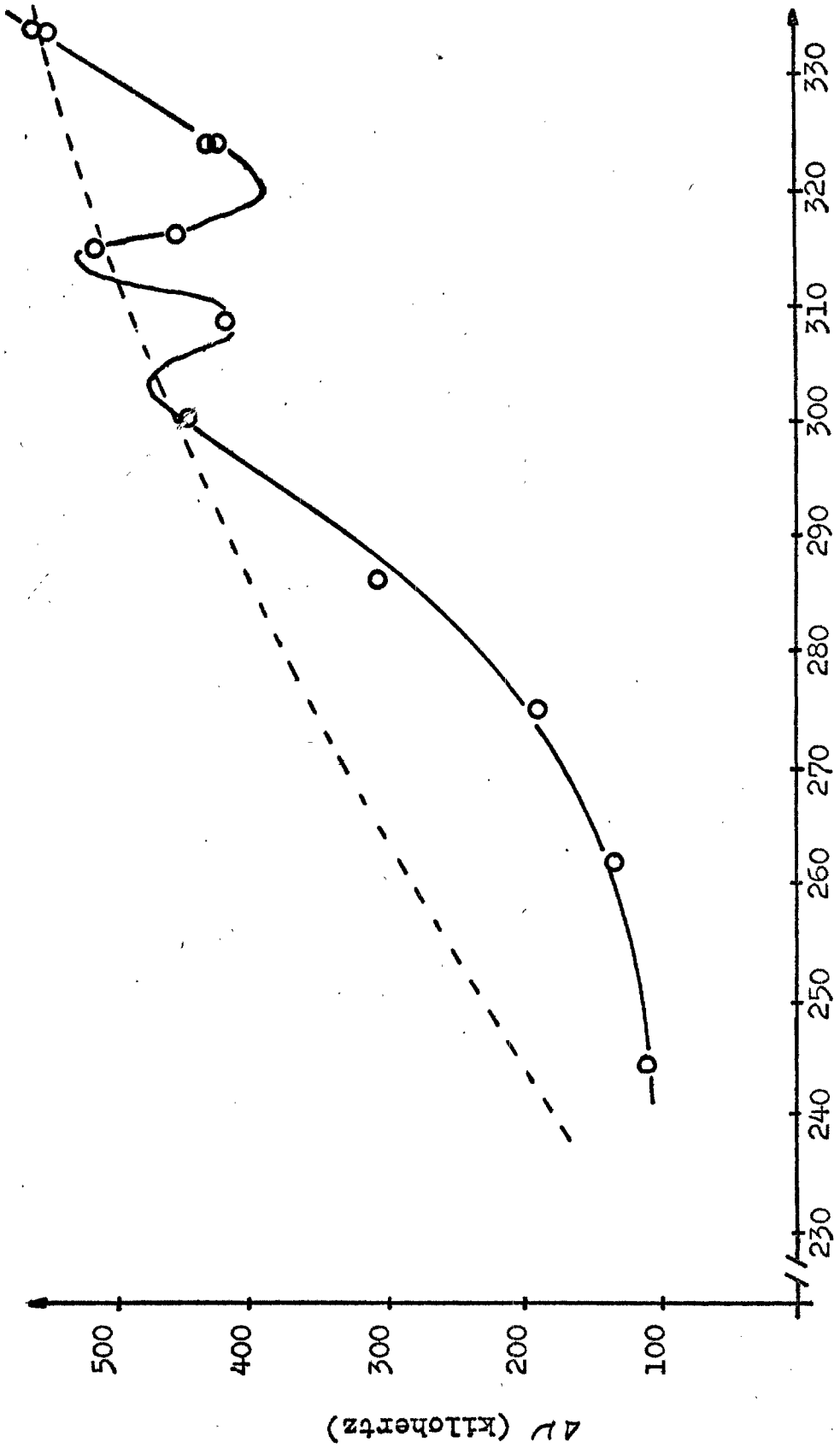

Fig. 20 -- Temperature dependence of line widths of the (8,6) inversion line of ammonia (first run). Dashed curve is best fit for no resonances.

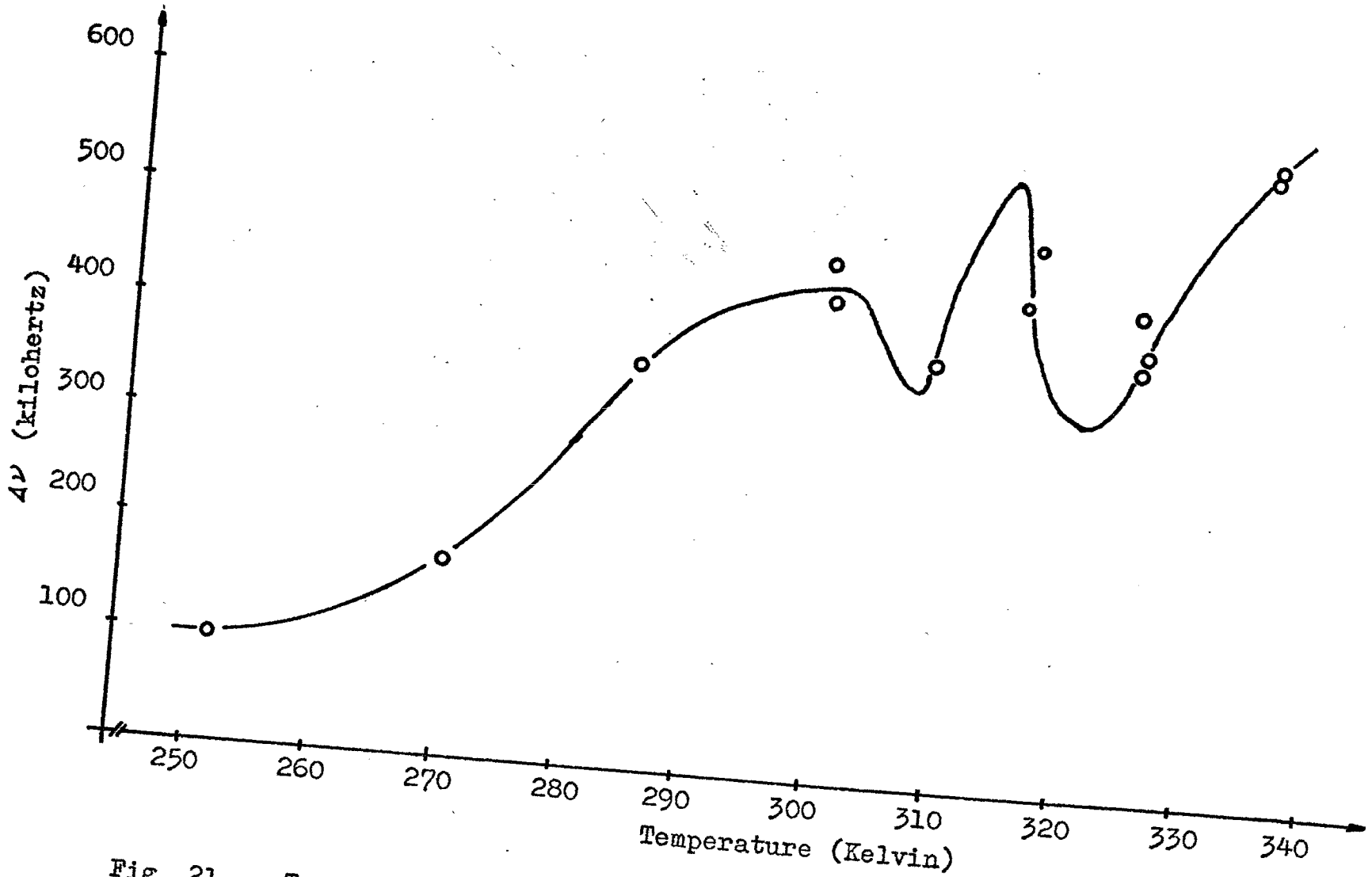

Fig. 21 -- Temperature dependence of line widths of the (8,6) inversion line of ammonia (second run).

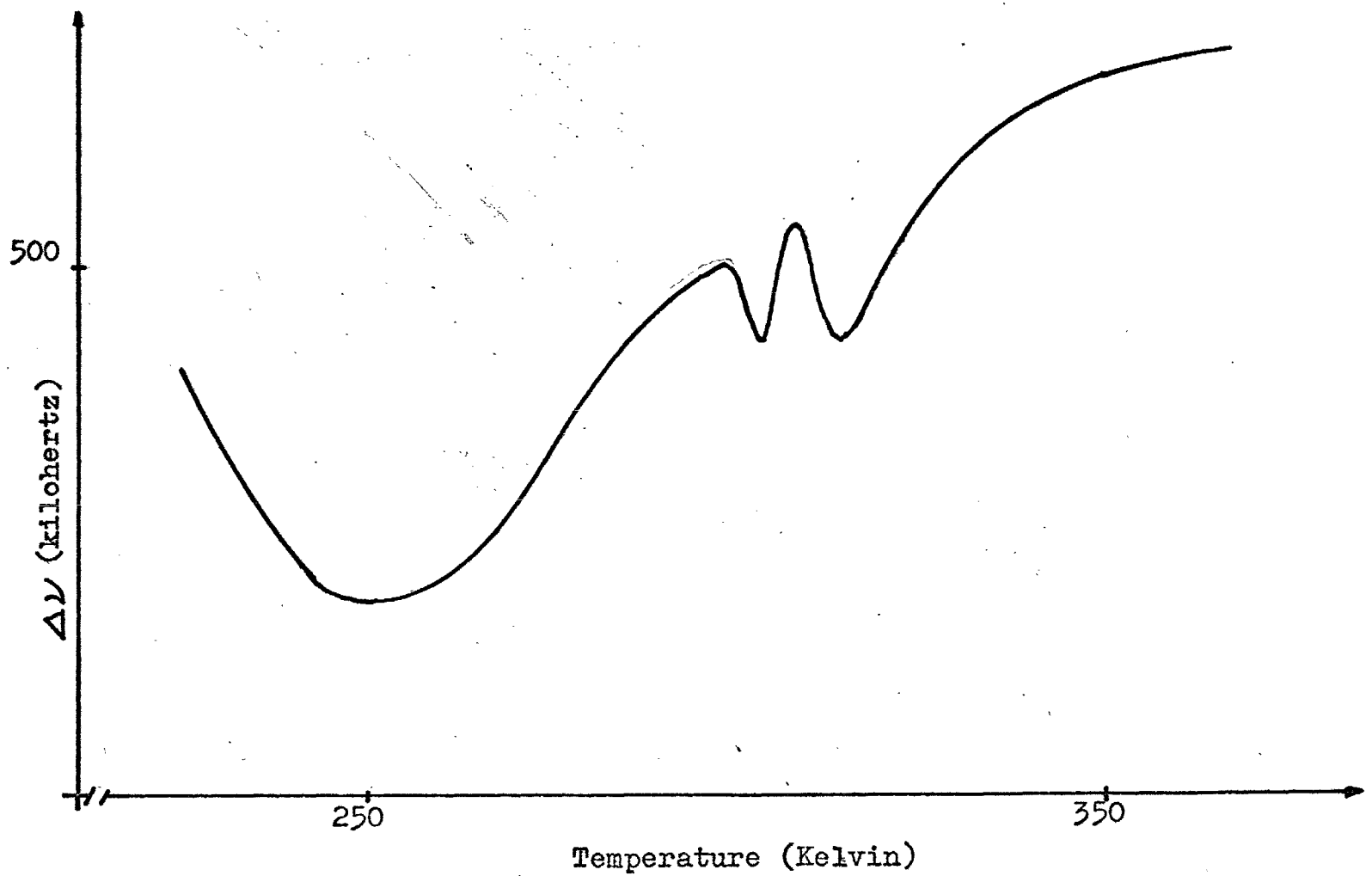

Fig. 22 -- Extrapolation of the experimental curve based on data obtained by Smith and Howard.

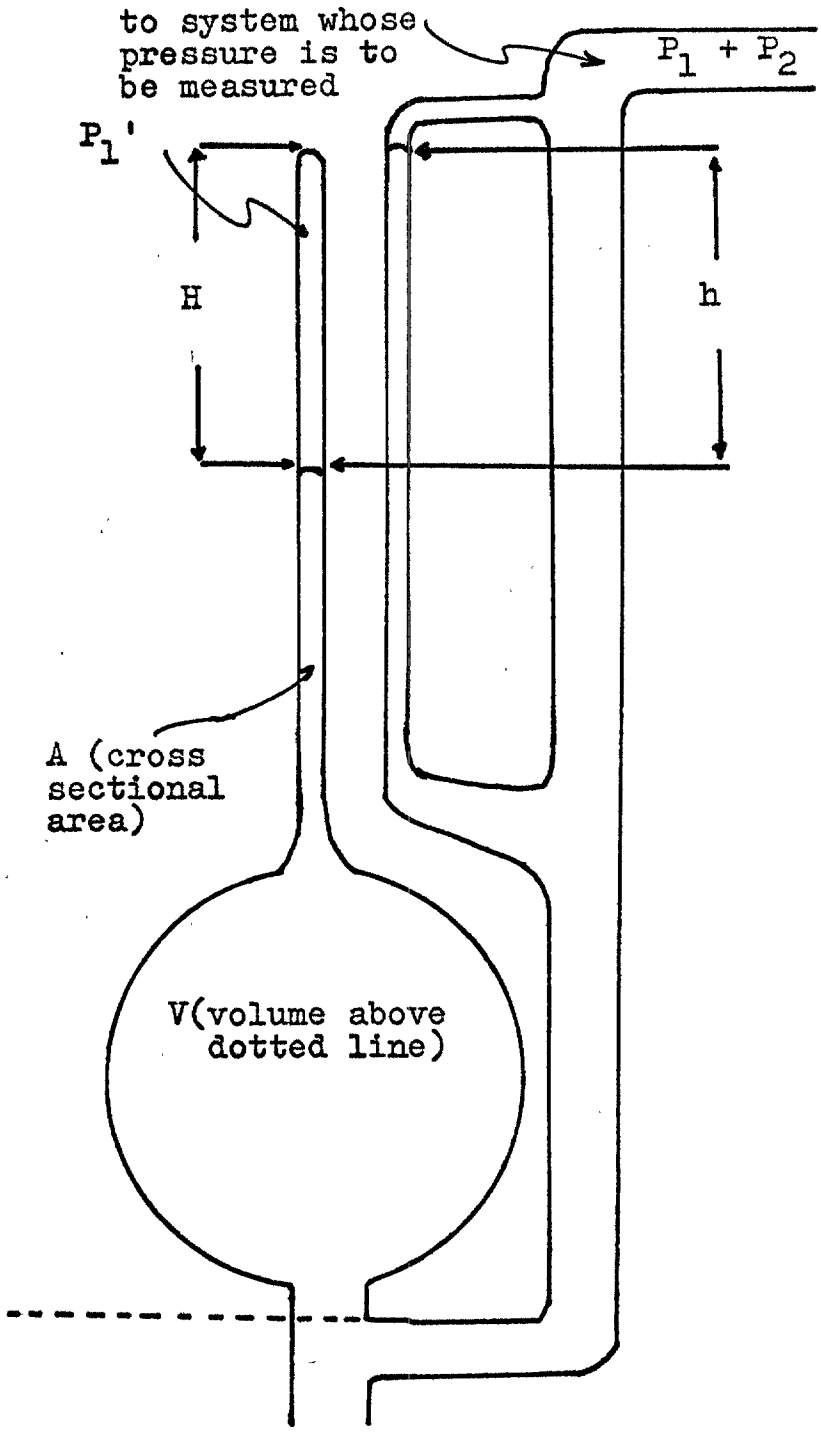

Fig. 23 -- Basic configuration of a McLeod gauge

TABLE I

INTERACTION POTENTIALS AND THE CORRESPONDING TEMPERATURE DEPENDENCES OF THE LINE WIDTH

Type of Interaction $\frac{1}{r^n}$	Potential Energy of Interaction	Temperature Dependence of
1. Dipole-dipole	$1/r^3$	1
2. Quadrupole-dipole	$1/r^4$	$T^{1/6}$
3. Quadrupole-quadrupole	$1/r^5$	$T^{1/4}$
4. Keesom alignment	$1/r^6$	$T^{3/10}$
5. Dipole-induced dipole	$1/r^6$	$T^{3/10}$
6. London dispersion	$1/r^6$	$T^{3/10}$
7. Quadrupole-induced dipole	$1/r^7$	$T^{1/3}$
8. Exchange force	exponential or high power of 1/r	-

TABLE II

PROJECTION OF DIPOLE MOMENT AN ANGULAR MOMENTUM AXIS AT VARIOUS TEMPERATURES

Projection, Debye	Temperature, Kelvin
.81360	350
.81351	330
.81342	310
.81333	290
.81325	270
.81319	250
.81314	230

TABLE III

TEMPERATURE CORRECTED MCLEOD GAUGE READINGS

Temperature (Kelvin)	Uncorrected Pressure (Microns)	Corrected Pressure (Microns)
334.6	13.616	13.697
299.6	24.590	24.584
270.3	24.475	25.336
252.0	25.429	37.105

BIBLIOGRAPHY

Books

Kemble, E. C., The Fundamental Principles of Quantum Mechanics, New York, McGraw-Hill, 1937.

Loeb, Leonard B., The Kinetic Theory of Gases, New York, Dover Publications Inc., 1961, 113.

Schiff, Leonard I., Quantum Mechanics, New York, McGraw-Hill, 1968, 413-414.

Townes, C. H. and Schawlow, A. L., Microwave Spectroscopy, New York, McGraw-Hill, 1955, 351.

Articles

Dennison, D. M. and Uhlenbeck, G. E., "The Two-Minima Problem and the Ammonia Molecule," Physical Review, XLI (August, 1932), 313-321.

Feeny, H., Lackner, H., Moser, Paul and Smith, W. V., "Pressure Broadening of Linear Molecules," The Journal of Chemical Physics, XXII (January, 1953), 79-83.

Johnson, C. M., "Line Breadth of OCS as a Function of Rotational Transition and Temperature," Physical Review, LXXXVII (August, 1952), 677-678.

Morgenau, Henry and Warren, Dana T., "Long Range Interaction Between Dipole Molecules," Physical Review, LI (May, 1937), 748-753.

Parsons, Ralph W. and Roberts, James A., "The Doppler Contribution to Microwave Line Widths," Journal of Molecular Spectroscopy, V (December, 1960), 458-473.

Rinehart, E. A., Legan, R. L., Lin, Chun C., "Microwave Spectrograph for Line Width Measurements," Review of Scientific Instruments, XXXVI (April, 1965), 511-517.

Smith, W. V., and Howard, R. R., "Microwave Collision Diameters II. Theory and Correlations with Molecular Quadrupole Moments," Physical Review, (July, 1950), 132-136.

_____, "Temperature Dependence of Microwave Line Widths," Physical Review, LXXVII (March, 1950), 840-841.

Smith, W. V., Lackner, H. A., and Volkov, A. B.,"Pressure Broadening of Linear Molecules II. Theory," The Journal of Chemical Physics, XXIII (February, 1955), 389-396.

Townes, C. H., "The Ammonia Spectrum and Line Shapes Near 1.25 - cm. Wave-Length," Physical Review, LXX (November, 1946), 665-671.

Unpublished Materials

Roberts, J. A., "An Improved Microwave Spectrometer for Line Width Measurements," (To be published) Review of Scientific Instruments.

_____, "Studies of Line Width of Microwave Spectra of Symmetric Top Molecules." Dissertation Abstracts, 1649-B, (1967).